Tellus (1986), *38A*, 333–365

On the extended-range predictability of large-scale quasi-stationary patterns in the atmosphere

By K. K. TUNG and A. J. ROSENTHAL, *Massachusetts Institute of Technology, Mathematics Department, Cambridge, MA 02139 USA*

(Manscript received March 21, 1984; in final form October 1, 1985)

ABSTRACT

A principal objective of this article is to establish theoretically the result that, contrary to some previously held beliefs, internal nonlinear processes (wave-wave and wave-mean interactions) among the large scales not likely to be the dominant mechanisms that lead to unpredictability of the low-frequency portion of the large-scale waves in the extra-tropical atmosphere. It is further argued that theoretically quasi-stationary long waves can probably be predicted at extended ranges if boundary forcings and tropical influence can be treated as known during the range of prediction.

The problem of long-range predictability of quasi-stationary long waves is studied here using a three-dimensional quasi-geostrophic channel model of the atmosphere, with lateral and lower boundary forcings prescribed. The low-frequency component of the flow is isolated by taking the running-time mean with an averaging period taken to be longer than the typical lifecycle of synoptic-scale baroclinic waves. When this period is chosen to be 10 days or longer, it is found that the evolution of the large-scale flow is not governed by a regular initial-value problem and detailed information of the initial condition is not "remembered' by the quasi-stationary waves beyond the predictability limit for the atmosphere as a whole. Instead, it is found that the extended-range evolution of the stationary waves responds to the corresponding evolution of the zonal index, which measures the total zonal geostrophic angular momentum in the channel. Some issues of theoretical predictability, such as the effect of small errors in the initial condition and of small uncertainties in our knowledge of the transient eddy fluxes, are addressed. It is argued that, since the evolution of the zonal index is found to be governed by a remarkably simple first order nonlinear differential equation of a single scalar function of time, whose solution has predictable properties, the quasi-stationary long waves, whose evolution is determined by the prognostic information contained in the zonal index, are perhaps also predictable beyond the "predictability limit".

1. Introduction

It is generally accepted that skillful forecasts of the instantaneous weather in detail at sufficiently long range ($\gtrsim$10 days) may be impossible (Lorenz, 1965, 1982; Smagorinsky, 1969). The question to be addressed here is: Can certain large-scale patterns be predicted at extended ranges if instantaneous information is not required (Charney, 1960)?

A capability to predict just the quasi-stationary long wave patterns would still be enormously useful for long-range weather forecasting even though it is the synoptic waves which comprise the daily weather. If, for example, the persistent large-scale ridge over the west coast of North America (as occurring during the winters of 1976/1977 and 1983/84) could have been predicted, one should have been able to infer with some confidence that the states east of the Rockies would experience colder winters due to the northerly flow component induced by the anticyclone, although the passage of individual storms over a particular locality would not have been predicted.

The task of extended range prediction is seen to be as much one of deciding *what* best to predict as *how* to predict it.

Loss of predictability for the atmosphere as a

whole occurs as the result of many factors. The atmosphere is highly unstable, especially in the synoptic scales. Inherent uncertainties initially present in an atmospheric state as observed, no matter how small, will, given long enough time, grow to dominate the flow field. Atmospheric motion is also nonlinear and rich in scales. Our uncertainty about physical processes at some scales will introduce errors in our prediction of the motion as a whole. And these errors may grow, leading again to a loss of predictability.

Loss of predictability for the atmosphere as a whole does not necessarily mean that information on the stationary long wave component of the flow is entirely lost. Unlike the synoptic waves, which are largely self-excited (through barotropic and baroclinic instabilities, for example), quasi-stationary waves in our atmosphere are mostly forced, by topography and stationary heating. As forced waves, their evolution is probably not as dependent on the details of the initial condition as is the evolution of the synoptic waves. In other words, it is likely that the quasi-stationary long waves do not have to "remember" much from their initial condition to know their evolutionary direction. Nonetheless it is also likely that some general quantity characterizing an initial condition is remembered by these waves; otherwise their large variability in model runs with fixed boundary conditions but different initial conditions cannot be easily explained in a deterministic manner.

A nonlinear quasi-geostrophic theory of forced quasi-stationary waves in three-dimensions is formulated here with the purpose of finding out how prognostic information in stationary waves is carried along in time. Equations for the quasi-stationary long waves are obtained by averaging the quasi-geostrophic equation in time in a running mean over a period t_T which is chosen to be greater than a few synoptic periods. Based on these equations, we ask the question: What do quasi-stationary long waves "remember" of their initial condition? It is found that even beyond the so-called predictability limit, determined mainly by the loss of predictability of the synoptic waves, prognostic information which determines the evolution of the quasi-stationary waves from one point in time to another is contained in a more robust mean quantity called the zonal index, which measures the total zonal geostrophic angular momentum in the westerly region. It is this quantity that the stationary waves remember over time and it is this quantity that is needed to characterize and to predict the state of the quasi-stationary waves (assuming that diabatic heating, transient eddy flax and boundary forcings are prescribed). It is shown that the zonal index satisfies a surprisingly simple first order ordinary differential equation. This equation can be used to predict its evolution if the mountain torque due to the stationary waves is known. Thus the equation for the zonal index is coupled to the equations for the stationary waves. However, as just mentioned, the prognostic variable for the stationary waves is contained in the zonal index itself. Consequently, as a prognostic equation, the zonal index equation is closed. It is a first order differential equation for one variable. It will be shown that such an equation has the theoretical property that its solution is predictable if boundary forcings, such as mountain heights, tropical forcing and diabatic heating, are prescribed.

If the evolution of the zonal index from an initial condition is predictable, the arguments to be presented in Section 3 then suggest that the evolution of the quasi-stationary waves is also predictable, provided that the latter are defined through the running time mean with the averaging period chosen so that the advection of the time-mean wave potential vorticity is much larger than the time rate of change of the time-mean wave potential vorticity. Under such a condition, the evolution of the quasi-stationary waves is "forced" by the evolution of the zonal index instead of developing independently from given initial conditions. As the zonal index varies, the quasi-stationary waves "adjust" their amplitudes and phases in response. For example, if in its evolution the zonal index passes through a value which is favorable for the response of wave number 2, then that particular wave will respond by adjusting its amplitude from a previous nonresonant value and equilibrating within an Ekman damping time τ_E to the new resonant value. Although the transient adjustment within τ_E (as discussed by Tung and Lindzen (1979a) for the linear case) is masked by our time averaging, the time-variable behavior of the quasi-stationary waves still manifests itself through the variability of the "adjusted" wave amplitude appropriate for the zonal index at that time.

Since we are mainly interested in the quasi-stationary long waves in midlatitude regions in the

atmosphere, tropical influence is specified in our model instead of interactively calculated. Similarly, surface heating is treated as a forcing term instead of calculated with a coupled atmosphere-ocean model. Our present results suggest that tropical influence is a major source of low-frequency variability of the large-scale extra-tropical waves and that an understanding of the coupling between the tropics and extra-tropical atmosphere is vital in long-range weather prediction.

2. Model framework

It is not the purpose of the present paper to make a definitive determination of how predictable the stationary waves in the real atmosphere are. Instead our focus is to isolate and study some possible mechanisms that can contribute to loss of predictability of the large-scale flow. So in this sense our model is a mechanistic one (in contrast to general circulation models).

One of the frequently-quoted mechanisms that are thought to be responsible for the loss of predictability of the atmosphere is nonlinear wave-wave and wave-mean interactions. This is an internal mechanism in the sense that it operates even in the absence of any changes in the external forcings. For example, one can construct a nonlinear model of midlatitude flows by considering a closed midlatitude channel with rigid lateral boundaries, with fixed diabatic heating and prescribed sea-surface temperatures. Although the coupling between the tropics and midlatitudes, in addition to couplings between the atmosphere and the oceans, are ignored, this simplified model of the atmosphere is still capable of possessing unpredictable behavior arising from nonlinear interactions between the synoptic and the large scales, as demonstrated by Reinhold and Pierrehumbert (1982) with a 2-layer model, and by Lorenz (1963) with an even more simplified model. An additional mechanism contributing to the variability of the atmosphere was suggested by Charney and DeVore (1979). This involves the interaction of large scale waves with the mean flow through the action of the mountain torque generated by the waves, which are themselves generated by the flow over a fixed mountain. The accompanying "form drag instability" is one possible contributor to the loss of predictability of the atmosphere as it acts to destabilize its equilibrium states.

We attempt in this paper to show using our mechanistic model that if one considers only the predictability of the quasi-stationary waves by filtering out the higher frequency, more chaotic, synoptic scale waves, the mechanisms of large-scale wave-wave and wave-mean flow interactions by themselves probably will not lead to the unpredictability of the quasi-stationary component of the flow. The effect of interactions between the stationary long waves and the higher frequency synoptic scale waves is treated less consistently as our model model does not predict the synoptic-scale transient waves. Instead the transient wave fluxes are prescribed in our model. By performing *sensitivity* studies using observed distributions and amplitudes (and double the observed amplitudes) of the transient eddy fluxes, we argue that these also are not likely to lead to unpredictability of the stationary long waves, unless our uncertainty of the magnitude of the transient eddy fluxes is 100% or more of the climatological magnitudes of these fluxes. We suggest that some previous model results probably have exaggerated the importance of the influence of the synoptic scales on the large-scale stationary waves by being in an unrealistic part of the parameter regime.

Thus it is to be understood from the beginning that the scope of our model is quite limited as we do not predict: (a) tropical forcing of the midlatitude atmosphere, (b) diabatic heating, and (c) transient eddy fluxes. These are prescribed functions of space and time in our model. We study only the variability of mid-latitude stationary long waves as they respond to these (prescribed) forcings.

We consider *nonlinear quasi-geostrophic* flows with small Rossby and Ekman numbers in a channel bounded by latitudes θ_1 and θ_2. At the channel boundaries the meridional velocity of the quasi-stationary quasi-geostrophic waves is required to vanish. Tropical forcing of midlatitude stationary waves is prescribed at the channel boundary in terms of the zonal mean Hadley circulation $(\bar{v}, \bar{w})$ (which is ageostrophic and so is not constrained by the aforementioned boundary condition), and the transient eddy fluxes of heat and momentum from the tropics (also not constrained by that boundary condition).

We shall adopt the definition for the zonal index, U, as "the net west-to-east geostrophic component of wind speed between latitudes θ_1 and θ_2 around the northern hemisphere". This definition is taken

essentially from Namias (1947), except that he specified θ_1 to be 35° N and θ_2 to be 55° N. We shall choose here θ_1 and θ_2 to be the channel boundaries for the quasi-stationary component of the flow and take $\theta_1 < \theta < \theta_2$ to contain the westerly wind belt, so near the surface typically $20° < \theta_1 < 30°$ N and $60° \text{ N} < \theta_2 < 90°$ N in winter. Thus

$$U(x,z,t) \equiv \frac{1}{y_2 - y_1} \int_{y_1}^{y_2} u_0(x,y,z,t)\, dy, \tag{2.1}$$

where

$$y \simeq a\theta,$$

$$z \equiv H_0 \ln\left(\frac{p_{00}}{p}\right), \tag{2.2}$$

and u_0 is the flow velocity in the eastward direction at the lowest order in Rossby number. The scalings in terms of Rossby number are given in Appendix A for the dimensionless equations; here we shall proceed to use the results in dimensional form.

Using geostrophy (A.9), one can see that

$$U = \frac{1}{(y_2 - y_1) f_0} [\Phi_0(x,y_1,z,t) - \Phi_0(x,y_2,z,t)]. \tag{2.3}$$

(Φ_0 is the geostrophic component of the geopotential). That is, the zonal index is given by the difference in geopotential height at two points separated by latitude.

Since we are not interested in the short term variations of the zonal index, we will consider only the running-time mean of U, defined by

$$\hat{U} \equiv \frac{1}{t_T} \int_{t-t_T/2}^{t+t_T/2} U\, dt, \tag{2.4}$$

where t_T is an averaging period suitably chosen to be longer than the life cycle of the synoptic scale disturbances. This approach is consistent with the original procedure adopted by Rossby and collaborators (1939), who used 5-day means of the zonal mean pressure at different latitude circles to construct "simple indices to the intensity of the general zonal circulation of the northern hemisphere" and found that such quantities on several occasions showed "marked trends ... persisting through several weeks". We shall, however, choose t_T to be longer than their 5 days in order to obtain more stable statistics on the transient eddies.

In this paper, the term, "quasi-stationary component" of the flow refers to the running-time mean (defined in (2.4)) of the flow quantity. [Note that the formulation to be presented will not be altered if a low-pass filter is used instead of the running-time mean]. "Quasi-stationary waves" are also objectively defined in the same manner. For example, the meridional velocity of the *quasi-stationary geostrophic waves* is given by $\hat{v}_0$. (Recall that the subscript 0 denotes the geostrophic component.) Thus, the lateral boundary condition mentioned earlier can be expressed as:

$$\hat{v}_0 = 0 \qquad \text{at } y_1 \text{ and } y_2 \tag{2.5}$$

with $v - \hat{v}_0$ specified at these two latitudes.

The continuity equation (A.10), together with the boundary condition (2.5), implies that the time-averaged zonal index, $\hat{U}$ is independent of longitude, i.e.

$$\frac{\partial}{\partial x} \hat{U} = 0. \tag{2.6}$$

Since our model is nonlinear, a lateral boundary condition is needed for the mean flow as well. Consistent with our intention to prescribe both the transient eddy fluxes of heat and the zonal mean Hadley circulation $(\hat{\bar{v}}, \hat{\bar{w}})$ at the channel boundaries, we shall prescribe the zonal mean temperatures at y_1 and y_2 as a function of height and time. In particular, the quantity

$$\Delta T^* \equiv \hat{\bar{T}}(y_1,z,t) - \hat{\bar{T}}(y_2,z,t) \qquad \text{is prescribed.} \tag{2.7}$$

That this is self-consistent with the wave-mean interactions in our model will be discussed in Appendix B. It is perhaps of interest to note that a specification of the temperature difference at the model boundaries was also adopted in the formulation of the cellular convection problem which Lorenz (1963) studied. He found unpredictable solutions in some parameter regimes. It therefore appears that the condition (2.7) does not preclude by itself the possibility of unpredictability in our model, although it is perhaps more satisfying to calculate in the model the boundary temperatures themselves as well. This, however, will require a credible model for the tropical atmosphere and will thus be beyond the scope of the present work.

3. What is remembered?

What do stationary long waves remember beyond the "predictability limit"? The term "predictability limit" is usually referred to as the period beyond which weather cannot be predicted *in detail* in any practical manner from a given initial condition. It is obvious that for extended-range prediction beyond the predictability limit one should not seek to predict the weather in detail, but should instead focus attention on an average quantity that can characterize the flow in some general sense. We will show here that since the quasi-stationary long waves, which determine the general large-scale weather pattern, remember only the zonal index, the predictability of the former is intimately tied to the predictability of the latter.

For large-scale waves in midlatitudes, which are quasi-geostrophic, the governing equation is the following pseudo-potential vorticity equation:

$$\frac{\mathrm{D}}{\mathrm{D}t}[P\Psi + f] = f_0\left(\frac{\partial}{\partial z} - \frac{1}{H_0}\right)(Q/\Gamma), \tag{3.1}$$

where

$$P \equiv \nabla^2 + \frac{H_0 f_0^2}{R}\left(\frac{\partial}{\partial z} - \frac{I}{H_0}\right)\frac{\partial}{\partial z}\frac{1}{\Gamma},$$

$$\frac{\mathrm{D}}{\mathrm{D}t} \equiv \frac{\partial}{\partial t} + J[\Psi,] = \frac{\partial}{\partial t} + \boldsymbol{u}_0 \cdot \nabla$$

$$J[\Psi,] \equiv \boldsymbol{k} \times \nabla\Psi \cdot \nabla, \qquad \Psi \equiv \Phi_0/f_0,$$

$$f \equiv 2\Omega \sin\theta \qquad \text{and} \qquad \Gamma \equiv \frac{\mathrm{d}}{\mathrm{d}z} T_0(z)$$

$$+ \frac{R/c_p}{H_0} T_0(z).$$

The lower boundary condition at the top of the Ekman layer, z_1, is (see Tung (1983))

$$-\frac{f_0 H_0}{R\Gamma}\frac{\mathrm{D}}{\mathrm{D}t}\Psi_z + \frac{f_0}{g}\frac{\partial}{\partial t}\Psi = J[\Psi, h]$$

$$+ \frac{H_0}{f_0}\frac{1}{\tau_E}\nabla^2\Psi - Q(z_1)/\Gamma. \tag{3.2}$$

The first term on the right-hand side of eq. (3.2) represents nonlinear flow over and around topography $h(x, y)$, and the second term on the right is the Ekman pumping arising from viscous mass convergence inside the Ekman boundary layer. τ_E is the Ekman damping time parameter given by (Charney and Eliassen, 1949).

$$\tau_E = H_0\left(\frac{2}{v_E f_0}\right)^{1/2}, \tag{3.3}$$

where v_E is the bulk eddy viscosity.

The equations are then time-averaged over the synoptic period with the purpose of obtaining an equation for the large-scale *quasi-stationary* waves. This yields

$$J[\hat{\Psi}, P\hat{\Psi} + f] = f_0\left(\frac{\partial}{\partial z} - \frac{1}{H_0}\right)\hat{Q}/\Gamma - \mathrm{TEP}, \tag{3.4}$$

where

$$\mathrm{TEP} \equiv \hat{J}[\Psi'', P\Psi''] \tag{3.5}$$

is the transient eddy flux convergence of potential vorticity, with $(\cdot)''$ denoting the deviation from the running-time mean $(\hat{\cdot})$, over an interval t_T, where t_T is an averaging period which should be longer than the life cycle of synoptic waves. (Its actual value should be chosen to make the transient eddy flux terms such as TEP well-behaved in time. A period of a month is probably sufficient for this purpose but shorter periods, such as 10 days, may also be adequate as long as t_T is longer than a few life cycles of the "random" disturbances.)

The lower boundary condition becomes, under the same time-averaging,

$$J\left[\hat{\Psi}, \left(\frac{f_0 H_0}{R\Gamma}\hat{\Psi}_z + h\right)\right] + \frac{H_0}{f_0}\frac{1}{\tau_E}\nabla^2\hat{\Psi} - \hat{Q}(z_1)/\Gamma$$

$$+ \mathrm{TEH} = 0, \qquad \text{at} \qquad z = z_1 \tag{3.6}$$

where

$$\mathrm{TEH} \equiv \hat{J}\left[\Psi'', \frac{f_0 H_0}{R\Gamma}\Psi_z''\right]$$

is the transient eddy heat flux convergence. These transient eddy fluxes presumably include the effect of baroclinic cyclones on the time-mean stationary waves (Gall et al., 1979; Hansen and Chen, 1982; Hansen and Sutera, 1984; Egger and Schilling, 1984). They should also include the effect of travelling waves on the stationary waves, although this latter effect is likely to be small for the free "normal-mode" travelling waves, since TEP and TEH can be shown to vanish for a single neutral mode.

In arriving at the time-mean equations, the slow time variation term, $\partial P\hat{\Psi}/\partial t$, is dropped in (3.4), since it is negligible compared to the advection of wave potential vorticity by the time-mean zonal flow, and $(\partial/\partial t)\ (f_0H_0/R\Gamma)\hat{\Psi}_z$ is dropped in (3.6) when compared with the mean temperature advection term. This is justified if the parameter

$$\varepsilon \equiv \frac{(1/t_T)}{(\hat{u}_0 k)} \tag{3.7}$$

is small. Here k is a typical wave-number for the quasi-stationary waves and so $1/(k\hat{u}_0)$ measures the advection time scale, which is typically smaller than the synoptic period. For example, a wave-number two wave (with $k = 2/a \cos\theta_0$) in a 20 m/s wind gives an advection time scale of ~1 day, which can be considered to be small compared to 10 days or more for t_T. A more formal derivation is given in Appendix A.

It would appear at this point that the appropriate governing equations for the running-time-mean flow, (3.4) and (3.6), are not prognostic and so cannot be used to predict the evolution of the quasi-stationary waves. Opsteegh and van den Dool (1979) encountered the same situation in their diagnostic study of the running-time-mean flow over northwestern Europe. They concluded that "the system of time-averaged equations has no capability of describing the evolution of the atmosphere from one specific mean state to another mean state in the future". They regarded the low-frequency variability of the time-mean atmosphere to be entirely determined by the second order transient eddy forcing terms (TEP and TEH in our equations), and therefore the parameterizations of these transient eddy flux terms have to be extremely accurate if the time-mean equations are to be used for the purpose of long-range prediction, a rather pessimistic prospect.

This does not turn out to be the case, because prognostic information is available at the leading order in ε through the lateral boundary condition, which has not been discussed so far.

The lateral boundary condition, (2.5), that the time averaged, geostrophic part of the meridional velocity, $\hat{v}_0 = \partial\hat{\Psi}/\partial x$, vanishes at y_1 and y_2 translates into the following condition for the stream function:

$\hat{\Psi}$ = a "constant" (independent of x) at $y = y_1$, and
$\hat{\Psi}$ = another "constant" at $y = y_2$.

In fact, the difference in the "constant" values of the stream function at y_1 and y_2 gives the total flow rate through the channel and hence measures the zonal index. Thus, one should specify as a boundary condition,

$$\hat{\Psi}|_{y_2} - \hat{\Psi}|_{y_1} = -\hat{U}(z,t)\cdot(y_2 - y_1). \tag{3.8}$$

This is how prognostic information enters into the time-mean wave equation to leading order in ε. Without (3.8), the system of time-mean equations with (2.5) as the lateral boundary condition is not properly posed, and admits an infinitude of solutions.

Since a time derivative term is absent from the equations for the quasi-stationary long waves ((3.4) and 3.6)), the long-term evolution of the stationary waves is not governed by a normal Initial-Value Problem, and the details of the initial condition are not "remembered". Strictly speaking, information concerning the details of the initial condition is still contained in the equation in the terms TEP and TEH. However, because these transient eddy terms are dominated by the unstable baroclinic waves, information concerning the evolution of the quasi-stationary long waves from an initial condition is gradually degraded and eventually lost for practical purposes after a life cycle of the baroclinic eddies ($\gtrsim t_T$).

Nonetheless, there is still considerable variability (with respect to time) in the quasi-stationary waves as a result of the time-dependent forcing for the system (3.4), (3.6) and (3.8) by the zonal index $\hat{U}(z,t)$.

If we regard the transient baroclinic eddy fluxes TEP and TEH as more or less random in time, and if their effect on the stationary waves predominates over that of the more systematic variations of $\hat{U}(t)$ and $\hat{Q}(t)$, then the system (3.4) and (3.6) would behave like a stochastic problem and the solution can be considered unpredictable, except perhaps statistically. We will argue in this article that this is not likely to be the case and that the evolution of the stationary long waves is governed largely by the *systematic* evolution of the zonal index.

In any case, since heating and transient eddy fluxes are assumed to be prescribed in the present model, the stationary waves are in principle determined once the zonal index, $\hat{U}(t)$, is known. Thus the evolution of the quasi-stationary long waves is governed by the evolution of the zonal index.

Since the stationary wave solution can be treated as a functional of $\hat{U}(t)$, any wave property, such as the *mountain torque* generated by the forced stationary waves, is also a functional of $\hat{U}(t)$. This result will be used in the next section to close the zonal index equation.

4. Evolution of the zonal index

The prognostic equation for u_0, and hence the zonal index, is given at the first order in Rossby number by the following nonlinear momentum equation, valid for $y > y_1$, and above the Ekman boundary layer (see Appendix A):

$$\frac{\partial}{\partial t} u_0 + u_0 \frac{\partial}{\partial x} u_0 + v_0 \frac{\partial}{\partial y} u_0 - \beta y v_0 - f_o v_1 = -\frac{\partial}{\partial x} \Phi_1, \tag{4.1}$$

where the subscript-1 quantities refer to the correction at the first order in Rossby number to the corresponding subscript-0 ones. At this order in Rossby number, the continuity equation is

$$\frac{\partial}{\partial x} u_1 + \frac{\partial}{\partial y} v_1 = -\frac{1}{\rho_0} \frac{\partial}{\partial z} (\rho_0 w_1) \tag{4.2}$$

with $\rho_0(z) \equiv \rho_0(0) e^{-z/H_0}$, and w_1 being the leading term in the vertical velocity in log-pressure coordinates.

Taking the meridional integral of (4.1) and recalling from (2.6) that $\hat{U}$ is a zonal mean quantity, one finds that

$$\frac{\partial}{\partial t} \hat{U} = \frac{f_0}{y_2 - y_1} \int_{y_1}^{y_2} \hat{v}_1 \mathrm{d}y + \frac{1}{y_2 - y_1} \widehat{\overline{u_0 v_0}}\Big|_{y_2}^{y_1}, \tag{4.3}$$

where the overhead bar denotes zonal average, and "$\widehat{\ }$" denotes time average and $\partial \hat{U}/\partial t$ is understood to mean $[\hat{U}(t + \frac{1}{2}t_T) - \hat{U}(t - \frac{1}{2}t_T)]/t_T$, i.e. the slow time derivative of $\hat{U}$. Let

$$\langle (\quad) \rangle \equiv \frac{1}{\rho_0(z_1) H_0} \int_{z_1}^{\infty} \rho_0(z) (\quad) \mathrm{d}z \tag{4.4}$$

be the vertical density-weighted average of ( ), where z_1 denotes the top of the Ekman boundary layer. The continuity equation (4.2) yields

$$\langle \bar{v}_1 \rangle = \frac{1}{H_0} \int_{y_1}^{y} \bar{w}_1(y', z_1, t) \mathrm{d}y' + \langle \bar{v}_1(y_1) \rangle, \tag{4.5}$$

assuming

$$\rho_0(\infty) \bar{w}_1(y, \infty, t) = 0$$

for the *mean* vertical motion. Therefore, the evolution of the vertically integrated angular momentum in a channel is given by

$$\frac{\partial}{\partial t} \langle \hat{U} \rangle = \frac{f_0}{(y_2 - y_1) H_0} \int_{y_1}^{y_2} \int_{y_1}^{y} \hat{\bar{w}}_1(y', z_1, t) \mathrm{d}y' \mathrm{d}y + f_0 \langle \hat{\bar{v}}_1(y_1) \rangle + \frac{1}{y_2 - y_1} \langle \widehat{\overline{u_0 v_0}} \rangle \Big|_{y_2}^{y_1} \tag{4.6}$$

The first term on the right-hand side of eq. (4.6) is determined by the *lower* boundary condition (at the top of the Ekman layer). Since "free" waves by definition satisfy a homogeneous lower boundary condition, they do not directly affect the evolution of the zonal index. Only forced stationary waves enter into the right-hand side of eq. (4.6). (Nevertheless, forced waves themselves may be affected by the "free waves").

Since the *time-averaged* vertical velocity in log-pressure coordinates is the same as the corresponding quantity in height coordinates, and the latter is given at $z = z_1$ by the sum of mountain uplift plus Ekman pumping (see Tung (1983)), we have at $z = z_1$

$$\hat{\bar{w}} = \frac{\partial}{\partial y} \overline{\hat{v}_0 h} + \frac{H_0}{f_0} \frac{1}{\tau_E} \frac{\partial^2}{\partial y^2} \hat{\bar{\Psi}}. \tag{4.7}$$

When (4.7) is substituted into (4.6), one finds

$$\frac{\partial}{\partial t} \langle \hat{U} \rangle = \frac{1}{\tau_E} (U^* - \hat{U}(z_1)) + \mathscr{E}, \tag{4.8}$$

where

$$U^* \equiv \frac{\tau_E}{(y_2 - y_1)} \langle \widehat{\overline{u_0 v_0}} \rangle \Big|_{y_2}^{y_1} + \hat{\bar{u}}_0(y_1, z_1, t) + \tau_E f_0 \langle \hat{\bar{v}} \rangle|_{y_1} = \frac{\tau_E}{(y_2 - y_1)} \langle \widehat{\overline{u_0 v_0}} \rangle \Big|_{y_2}^{y_1} \tag{4.9}$$

and

$$\mathscr{E} \equiv \frac{f_0}{H_0 (y_2 - y_1)} \int_{y_1}^{y_2} \overline{\hat{v}_0 h}\,|_{z_1} \mathrm{d}y. \tag{4.10}$$

Here U^* represents the zonal momentum flux at the lateral boundaries of the channel by the transient eddy momentum fluxes and the time mean Hadley cell. $\mathscr{E}$ denotes the mountain torque. It

represents the torque on the total angular momentum of the atmosphere in the channel exerted by unequal pressure forces acting on the east and west sides of topographic elevations. This quantity is to be calculated separately using a model for the stationary waves.

The last two terms in (4.9) cancel each other (assuming the mean Hadley circulation at y_1 does not transport net mass across y_1) because $\langle \hat{v}_1 \rangle|_{y_1}$ represents the total mean meridional mass flow of the Hadley circulation *above* the Ekman boundary layer, while $(1/f_0\tau_E)\hat{\bar{u}}_0(y_1, z_1)$ turns out to be the return mass flow *inside* the Ekman boundary layer (see Appendix A).

4.1. Zonal momentum driving

Various values have been adopted for the zonal momentum driving term in barotropic models, which tend to assume, perhaps erroneously, that this term is of thermal origin and so cannot be determined consistently within the barotropic model. Our result suggests that the zonal momentum driving term in barotropic models (or in baroclinic models, for that matter) can be identified with U^* defined in (4.9), which is due to the momentum fluxes across the channel boundaries (see also Rambaldi (1982)). In previous barotropic and two-layer channel models, the term U^* is absent not because of the neglect of baroclinic effects, but because the model lateral boundaries are taken to be *closed*. The rigid boundary conditions used in those models:

$$v_0 = 0, \qquad v_1 = 0 \qquad \text{at } y_1 \text{ and } y_2$$

imply

$$U^* = 0.$$

A zero zonal driving term would lead to the conclusion that the zonally symmetric circulation (in the absence of mountains) would spin down to an equilibrium state with no net zonal flow at the "surface". To maintain net westerly flow in the channel, some authors have introduced a nonzero zonal momentum driving term in the vorticity equation, with its value assumed to be arbitrary as far as barotropic models are concerned. In some two-layer models, the zero-surface flow solution, the so-called Hadley regime, is circumvented by adopting a higher (perhaps unrealistic) parameter value for baroclinicity, which then leads to some surface flow through instability processes.

By adopting an *open* model in the present study, we now allow the transient eddy momentum fluxes and the mean Hadley circulation to act to maintain a net westerly flow inside the channel outside the planetary boundary layer. Since

$$U^* = \frac{\tau_E}{(y_2 - y_1)} \langle \widehat{\overline{u_0 v_0}} \rangle \Big|_{y_2}^{y_1} = \frac{\tau_E}{(y_2 - y_1)} \langle \widehat{\overline{u_0'' v_0''}} \rangle \Big|_{y_2}^{y_1}, \tag{4.11}$$

we see that the zonal momentum driving is determined by the net momentum flux convergence into the channel due to transient eddies. [In the real atmosphere, part of U^* is due to the equatorward flux of easterly momentum by the stationary long waves. In the present mechanistic model, U^* will be taken to be independent of the stationary long waves, by virtue of (2.5).] Observational studies (see, e.g. Lau (1979), Fig. 5e), show that the transient eddy momentum flux at the northern boundary ($\theta_2 > 60°$ N) is negligibly small compared to the transient eddy momentum flux at the southern boundary. For the purpose of comparing with Charney et al. (1981), we shall estimate U^* for $\theta_1 \simeq 30°$ N, although a more equatorward position for θ_1 may be more appropriate if U^* is to be considered as independent of the stationary long waves for the real atmosphere. Using Lau's data, we estimate that

$$U^* = \frac{\tau_E}{(y_2 - y_1)} \langle \widehat{\overline{u_0'' v_0''}}(y_1) \rangle \simeq 2\text{m/s}, \tag{4.12}$$

for a "climatological" atmosphere during winter, assuming $\tau_E \sim 6$ days. [In a primitive equation formulation, the momentum flux in U^* should have included a term due to the advection of $\hat{u}$ by the mean Hadley flow $\bar{v}$ (see Tung and Rosenthal (1985)). However, since $\bar{v} \sim 0$ at $\theta_1 \sim 30°$ N, the value estimated in (4.12) for U^* should also hold for the primitive equation case.] Allowing for interannual variability of the transient eddy fluxes and our uncertainty in the value of τ_E, a *range* of values for U^* from 2 m/s to 4 m/s, will be adopted in our sensitivity studies. [This range also seems to hold when θ_1 is chosen to be more equatorward than 30° N and into the Hadley circulation regime, when the primitive equation version of U^* is used.]

4.2. Vertical structure of the zonal index

From the thermal wind relation, we find that the vertical shear of the zonal index is determined by the zonal mean temperature difference between the two channel boundaries:

$$\frac{\partial}{\partial z}\hat{U} = \frac{R}{(y_2-y_1)H_0 f_o}[\hat{\bar{T}}(y_1,z,t) - \hat{\bar{T}}(y_2,z,t)]$$
$$\equiv \frac{R}{(y_2-y_1)H_0 f_0}\Delta T^*. \tag{4.13}$$

Since ΔT^* is prescribed by our lateral boundary condition (2.7), according to (4.13) the vertical shear of $\hat{U}$ is maintained by this temperature difference and so is a known function. The prescribed temperature difference ΔT^* plays an analogous role to that of the thermal driving term $\Delta\Theta^*$ in the two-layer model of Charney and Straus (1980). In a general circulation model one should in principle predict instead of prescribe ΔT^*, but this is beyond the stated scope of this paper. Nevertheless, we still need to demonstrate the internal consistency of our model formulation by showing that the specification of mean temperatures at the channel boundaries does not violate the principle of wave-mean flow interaction. This task is relegated to Appendix B.

It follows from (4.13) that the shear of the zonal index is *not* an unknown prognostic quantity and can be taken to be specifiable in our model. In other words, it is necessary only to predict the zonal index at (any) one level, say, at z_1; the zonal index at any other level can be calculated as

$$\hat{U}(z,t) = \hat{U}(z_1,t) + \frac{R}{(y_2-y_1)f_o H_0}\int_{z_1}^{z}\Delta T^*(z,t)\mathrm{d}z. \tag{4.14}$$

The above result should not be taken to mean that the vertical shear of the zonal flow does not change inside the channel (in fact we know it should change); only the *y-integral of the shear* over the channel does not change as a *result of wave-mean flow interaction.*

4.3. Prognostic equation for the zonal index

Through an integration by parts, one can express the vertically integrated quantity $\langle\hat{U}\rangle$ in terms of its "surface" value as

$$\langle\hat{U}\rangle = \hat{U}(z_1,t) + \Delta(t),$$

where

$$\Delta \equiv \frac{R}{(y_2-y_1)f_0}[\langle\hat{\bar{T}}(y_1) - \hat{\bar{T}}(y_2)\rangle]. \tag{4.15}$$

The zonal index equation (4.8) can now be written in terms of the surface zonal index, $U_0 \equiv \hat{U}(z_1,t)$, alone:

$$\frac{\partial}{\partial t}U_0 = \frac{1}{\tau_E}(U^\dagger - U_0) + \mathscr{E}, \tag{4.16}$$

where

$$U^\dagger \equiv U^* - \tau_E\frac{\partial}{\partial t}\Delta$$

is the zonal momentum driving for the surface flow. The mountain torque $\mathscr{E}$ is a function of the surface stationary wave amplitude, which in turn is a functional of $\hat{U}(z,t)$ as demonstrated in Section 3. Because of (4.14), the functional dependence of $\mathscr{E}$ on $\hat{U}$ can be written as

$$\mathscr{E} = \mathscr{E}(U_0, \Delta T^*).$$

Since ΔT^* and U^* are both prescribed in the present model, (4.16) is of the simple form of a first order nonlinear ordinary differential equation for U_0 only; i.e.

$$\frac{\mathrm{d}}{\mathrm{d}t}U_0 = F(U_0,t) \tag{4.17}$$

with

$$F(U_0,t) \equiv \frac{1}{\tau_E}(U^\dagger(t) - U_0) + \mathscr{E}(U_0, \Delta T^*(t)). \tag{4.18}$$

The autonomous form of (4.17) will be studied in the phase plane in Section 5, while the non-autonomous form will be discussed in Section 6.

5. Dynamical predictability

The term "dynamical predictability", as defined by Shukla (1981), refers to the predictability of the large scales in a dynamical model with fixed external forcings. For our model, this means fixed mean temperatures and fixed momentum fluxes *at the channel boundaries*, viz.

$$\frac{\partial}{\partial t}\Delta = 0, \qquad U^\dagger = U^*$$

independent of t; ΔT^* independent of t,

and so the zonal index equation becomes

$$\frac{\mathrm{d}}{\mathrm{d}t} U_0 = F(U_0). \tag{5.1}$$

This system is autonomous and can be studied very easily in the phase plane here.

Despite the existence of Picard's Theorem, which establishes the existence and uniqueness of solutions to the initial value problem (4.17), unpredictability in the solution may still arise for practical purposes in the presence of uncertainties in the initial condition, and in the transient eddy "forcing" terms TEP and TEH that determine the form of $F(U_0)$. These two issues will be addressed *separately*.

5.1. *Predictability in the presence of uncertainties in initial conditions*

To address specifically the question of unpredictability in the presence of uncertainties in initial conditions, we shall first treat the system (5.1) as deterministic by ignoring the uncertainties in the forcing terms (including TEP and TEH) and parameterized processes (such as the Ekman boundary layer formulation).

Such a system is said to be unpredictable if small differences in two initial states can lead to a large divergence in the behavior of the two solutions at large later times. We show here using the phase-plane method that such a situation is not generally the case for solutions of (5.1). Since the arguments to be presented are independent of the detailed form of the mountain torque, there is no need to specify a stationary wave model and no actual calculation is required at this point.

Fig. 1 is a *schematic* depiction of the behavior of $F(U_0)$ with and without the mountain torque. Since $F(U_0)$ is $\mathrm{d}U_0/\mathrm{d}t$, the flow in the portions of the diagram where $F > 0$ will be accelerating to larger values of U_0, and decelerating where $F < 0$. The *fixed points*, at which $F = 0$, are the so-called "equilibria". An equilibrium state for the zonal index is stable if the flow on the larger U_0 side is decelerating and the flow for smaller U_0 is accelerating. Otherwise the fixed point is an "unstable equilibrium".

In the absence of mountains, there is only one equilibrium, $U_0 = U^*$, which is stable. A flow with an initial condition of $U_0 \neq U^*$ will relax into this equilibrium state in Ekman damping time scales.

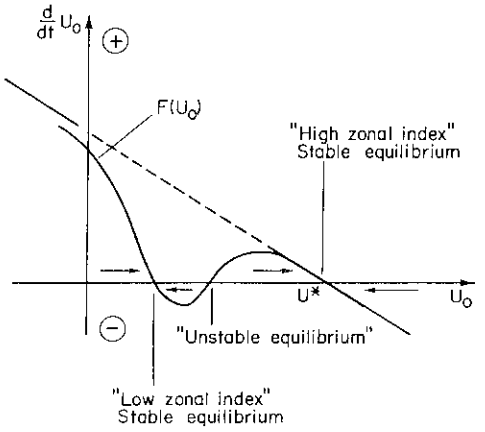

Fig. 1. A schematic phase diagram of $\mathrm{d}U_0/\mathrm{d}t = F(U_0)$ versus U_0 for the case when the mountain torque creates a large deceleration of the zonal index on the low side of U^*. The dashed straight line is $F(U_0)$ in the absence of mountain torque. One stable equilibrium exists at $U_0 = U^*$ for the no-mountain case, and three equilibrium points (two stable and one unstable) appear in the case with mountains. Arrows indicate the direction that U_0 tends.

In the presence of mountain torque, "dips" will be created in the (otherwise) straight line of the no-mountain case. These dips occur at the U_0's that give preferred responses to the stationary planetary waves (i.e. resonances). (Since the diagram is schematic only, only one dip is shown in Fig. 1. In general there are many dips associated with the resonances of various horizontal and vertical wavenumbers. In the presence of Ekman damping, only a couple of these are noticeable in reality.) If the additional deceleration associated with the mountain torque occurs where $U_0 < U^*$, multiple equilibrium points may be created. In Fig. 1, it is shown that two additional equilibrium points may be created by a mountain torque that dips once caused by a one-mode wave. One of the points, the so-called "subresonant equilibrium" point, is stable, while the other, the so-called "superresonant equilibrium" point, is unstable to the form drag instability according to the criterion mentioned above. These two, together with the so-called "high zonal index equilibrium", near U^*, are analogous to the well-known multiple equilibrium states found by Charney and DeVore (1979) and Charney et al. (1981) in severely truncated barotropic models. The choice of a large value for U^* (e.g. Charney et al. used $U^* \simeq 63$ m/s) in these models is partly

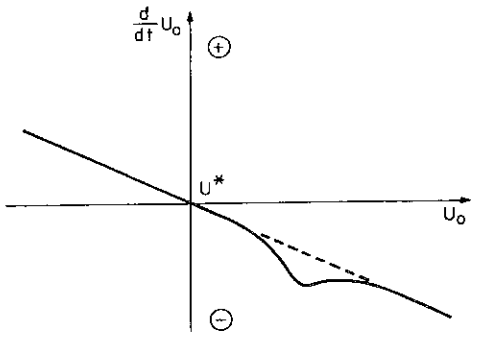

Fig. 2. A schematic phase diagram for the case when the mountain torque creates a deceleration of the zonal index on the high side of U^*, a predictable situation.

responsible for the situation depicted in Fig. 1 (i.e. dips occurring on the $U_0 < U^*$ side) occurring.

For the case when the resonance of the stationary planetary waves ocurs on the $U_0 > U^*$ side, as depicted in Fig. 2, there is only one equilibrium, located near U^*.

In general it can be shown that (5.1) possesses at least one stable fixed point which is bounded. Since

$$F(U_0) = \frac{1}{\tau_E}(U^* - U_0) + \mathcal{E}(U_0),$$

and

$$\mathcal{E}(U_0) \to 0 \qquad \text{as} \qquad U_0 \to \pm\infty,$$

we know that

$$F(U_0) \to -\frac{1}{\tau_E} U_0 \qquad \text{as} \qquad U_0 \to \pm\infty.$$

Therefore $F(U_0)$ is negative for large positive U_0 and positive for large negative U_0. It follows then that $F(U_0)$ must have at least one zero for some finite value of U_0, and that one of the zero-crossings of $F(U_0)$ must have a negative slope. This then proves the claim that there is a stable finite equilibrium point.

When there exists only one such equilibrium state, to which all solutions with different initial conditions will tend to as $t \to \infty$, the system is predictable. Then any error initially present will ultimately vanish.

When the system possesses two or more stable equilibria, a set of solutions will tend to one equilibrium, while a different set will tend to another equilibrium. In the example depicted in Fig. 1 all solutions whose initial U_0 is larger than the unstable fixed point will tend to the "high zonal index" equilibrium $U_0 \simeq U^*$, while all solutions whose initial U_0 is smaller than the unstable fixed point will ultimately tend to the "low zonal index" equilibrium, as indicated by the arrows. These behaviors are still considered predictable, except if the initial U_0 is near the unstable fixed point. At this point, two solutions whose initial conditions are arbitrarily close can diverge in two different directions. Although our model in principle permits the existence of multiple equilibria in an analogous manner as in the simple truncated barotropic models, we will show (in Section 7 and also in Tung and Rosenthal (1985)) that in practice only a single equilibria is found when severe truncation is not adopted. The situation is similar to that depicted in Fig. 2, which is predictable.

5.2. *Predictability in the presence of uncertainties in transient eddy fluxes.*

In addition to their explicit effect on the zonal index equation through the U^* term, transient eddy fluxes also affect the evolution equation indirectly via their effect on the stationary waves. That is, the form of the mountain torque calculated with and without the terms TEP and TEH in (3.4) and (3.6) is probably different. Since there are uncertainties in our knowledge of these transient eddy terms, predictability properties of the zonal index equation can be affected if these uncertainties are large enough.

However, the study of predictability is not concerned with large uncertainties in our knowledge of the governing equation, but with the growth of small errors introduced by small uncertainties. The system under consideration is said to be predictable if the errors in the solution remain small even at large times. An example of a "predictable" situation is depicted in Fig. 3, while Fig. 4 represents an "unpredictable" situation. To be "unpredictable", the errors in $F(U_0)$ introduced by our uncertainties in transient eddy fluxes not only have to be finite, but also *additional* equilibrium points (i.e. zeroes of $F(U_0)$) must be created by the errors, so that the ultimate destination of some of the solution in the phase-plane is altered. This is a more precise and stronger criterion for unpredictability than previously used.

Our experience with forced-damped systems such as (3.4) and (3.6) suggests that a small change

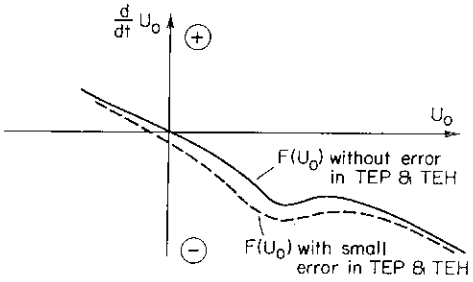

Fig. 3. A schematic phase diagram showing the effect of a small error in the transient eddy flux terms, TEP and TEH. A predictable situation.

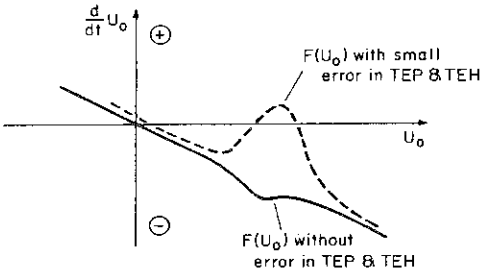

Fig. 4. Same as in Fig. 3 except for the unlikely case of a large deformation in the phase plane caused by a small error in the transient eddy fluxes, an unpredictable situation.

in the "forcing" terms TEP and TEH will produce only a small change in the solution, and consequently only a small change in the form of $F(U_0)$. The situation is similar to that depicted schematically in Fig. 3.

6. Predictability of the nonautonomous system and the effect of tropical influence

It should be noted that our conclusion from the previous section on the predictability of the zonal index depends to some extent on the fact that in our model the derived evolution equation for the zonal index is not a coupled set of nonlinear differential equations. Unpredictability can arise when a system has many degrees of freedom. In fact, chaotic behavior can result from deterministic equations for systems containing as few as three coupled first order ordinary differential equations for three scalars (Lorenz, 1963). In a model more complicated than the present one, in which interactive couplings of the tropical atmosphere and oceans to the midlatitude atmosphere are incorporated, the governing evolution equations for the system as a whole are likely to be coupled and the number of degrees of freedom is probably three or larger. Consequently unpredictable solutions cannot be ruled out.

The incorporation of interactive coupling between the midlatitude atmosphere and the tropical atmosphere, with the latter coupled to the equatorial oceans, has not been accomplished in the present model. Nevertheless, some assessment of the effects of tropical influence on the mid-latitude system can still be made with the lateral boundary forcing terms at θ_1 *prescribed* in accordance with observed atmospheric data. This is the approach that is adopted in the present paper.

With the momentum and thermal driving terms, $U^\dagger$ and ΔT^*, now as (prescribed) functions of time, the system (4.17) is no longer autonomous, and the word "equilibrium" is no longer meaningful. Although the nonautonomous system is no more difficult to solve numerically than the autonomous system, strictly speaking the phase-plane method discussed in Section 5 for the autonomous system no longer applies. While there exist some known pedagogical cases (i.e., one example is the "harvesting problem", in which a stepwise variation in time of the forcing function leads to a chaotic solution) which can lead to chaotic behavior in the solution of a deterministic nonautonomous equation, we have found from numerical integration of the zonal index equation that the behavior of the solution in the present case is still qualitatively the same as in the autonomous case provided that the forcing function, e.g. $U^\dagger(t)$, varies on a time scale longer than τ_E, the relaxation time of the system. In particular, the solution will still tend to the "equilibrium" point, $U_0 \sim U^\dagger(t)$, except now this point is shifting on a slow time scale.

In addition to the tropical momentum flux, heat fluxes from tropical disturbances can also affect the evolution of the zonal index by changing the *vertical shear* of the zonal index through the effects of transient eddy heat flux propagated northward and upward from the tropical region (Jacqmin, 1983). [Another mechanism, which is not treated

here, arises when conditions near the tropical zero-wind line cause changes in the equatorward fluxes of heat and momentum from the extra-tropical stationary long waves. Such a mechanism is excluded by our boundary condition (2.5).] The altered shear can cause significant changes in the responses of the stationary waves in the mid-latitudes (see, e.g. Tung and Lindzen (1979b)). The effect of such a change is to shift the dip in the mountain torque caused by the quasi-resonance of the planetary scale waves to lower or higher values of U_0.

The above discussion points to the manner through which the low-frequency *variability* of the stationary wave system can be affected by tropical disturbances. In our model with *prescribed* tropical forcing, the system is considered to be predictable if uncertainties in the tropical forcing do not lead to additional equilibria. While the creation of additional equilibria through the variation of ΔT^* is in principle a distinct possibility in baroclinic models (see the result of the two-layer model of Charney and Straus (1980)), we find that in the range of realistic parameters, only a single equilibrium of the large scale flow is present in our model. An explanation of the discrepancy between the present model and previous two-layer models will be discussed in more detail in the next section.

7. Some simple numerical experiments

To illustrate how ideas discussed in the previous sections can be synthesized in a numerical model of stationary waves, we shall discuss here results of three sets of experiments. In the first set the imposed temperature difference across the channel, ΔT^*, is prescribed to be zero. In the second set $\Delta T^*(z)$ is prescribed in accordance with observed temperature differences. Although our model is fully three-dimensional, the $\Delta T^* \equiv 0$ case behaves qualitatively similar to a barotropic model and thus can serve as a bridge in understanding our three-dimensional results in the context of previous work using barotropic models. To understand previous results based on two-layer models we perform a third set of calculations using constant values of ΔT^*. By increasing this parameter through a range of values, we hope to simulate some of the responses of solutions in two-layer models to increases in baroclinicity.

7.1. *Simplifying assumptions*

We assume that there exists an "upstream" region in some longitude band (somewhere in the western Pacific, say) in the atmosphere where zonal asymmetries in the time-mean flow vanish. This assumption is not always applicable to the real atmosphere; we will come back to this point later in this subsection. Evaluating the potential vorticity equation (3.1) upstream then yields

$$\frac{\partial}{\partial t} P\hat{\Psi}^{(u)} = \frac{f_0}{\rho_0}\frac{\partial}{\partial z}\rho_0 \hat{Q}^{(u)}/\Gamma - \mathrm{TEP}^{(u)}, \tag{7.1}$$

where the superscript "(u)" denotes upstream value. Since the quantities on the right-hand side of eq. (7.1) are to be prescribed in our model, we choose in this simple example the case where the mean heating term balances the transient eddy flux term, i.e.,

$$\frac{f_0}{\rho_0}\frac{\partial}{\partial z}\rho_0 \hat{Q}^{(u)}/\Gamma = \mathrm{TEP}^{(u)}, \tag{7.2}$$

so that eq. (7.1) implies

$$\frac{\partial}{\partial t}\left\{\frac{\partial}{\partial y}\hat{u}^{(u)} - \frac{f_0}{\rho_0}\frac{\partial}{\partial z}\hat{T}^{(u)}/\Gamma\right\} = 0 \tag{7.3}$$

Eq. (7.3) allows us to make the simplifying assumption that the *upstream shears* are invariant and so can be prescribed by the initial condition. Note that (7.3) does *not* give us the freedom to specify the magnitude of the upstream flow, $\hat{u}^{(u)}(y,z,t)$. That has to be determined in conjunction with the wave-mean flow interaction equations.

Assuming that the initial condition is one in which upstream flow has no meridional shear, we then have.

$$\hat{u}^{(u)} = \hat{u}^{(u)}(z,t) \qquad \text{for all } t \geqslant 0. \tag{7.4}$$

Thus the upstream flow is the same as the zonal index, which was defined to be the average of the zonal flow over the y-domain,

$$\hat{u}^{(u)} = \hat{U}(z,t). \tag{7.5}$$

The nonlinear perturbation equation is obtained by subtracting the upstream part (7.1) from the full potential vorticity equation, (3.1), resulting in

$$J[\hat{\Psi}, P\hat{\Psi} + f] = \frac{f_0}{\rho_0}\frac{\partial}{\partial z}\frac{\rho_0}{\Gamma}(\hat{Q} - \hat{Q}^{(u)}) - (\mathrm{TEP} - \mathrm{TEP}^{(u)}). \tag{7.6}$$

Only a simpler version of (7.6), obtained by ignoring the forcing terms on its right-hand side, is considered in this section:

$$J[\hat{\Psi}, P\hat{\Psi} + f] = 0. \tag{7.7}$$

In going from (7.6) to (7.7), we have ignored differential heating and Newtonian cooling, which will give rise to a nonzero $\hat{Q} - \hat{Q}^{(u)}$, and have also not included the effect of the zonally asymmetric part of transient eddy fluxes of potential vorticity on the stationary waves in the *interior* of the fluid. We will, however, retain the effect of the transient eddy flux of heat near the surface, which was found by Lau (1979) and Lau and Wallace (1979) to be more important. Ekman damping near the lower boundary provides the only dissipative mechanism in this simple example, and since the Ekman damping time scale is usually taken to be shorter than the Newtonian cooling damping time scale in the lower atmosphere, the neglect of the latter in our model does not appear to be detrimental to our overall problem, as far as the lower atmosphere is concerned. Assumptions (7.4) and (7.7) are made here to reduce the computer storage needed by our solution procedure by decoupling the vertical structure of the waves from their horizontal structures, and to facilitate imposing the appropriate upper boundary conditions (radiation or boundedness condition). The resulting gain in computing efficiency allows us to use very high vertical resolution, prompted by the recent claim by Jacqmin and Lindzen (1985) that insufficient vertical resolution in most existing models has led to spurious sensitivity of stationary wave response to mean wind configuration, a very undesirable defect for our purpose of studying wave variability.

Integrating (7.7) along a streamline and evaluating "the constant of integration" upstream using (7.5), we find

$$\nabla^2\hat{\Psi} + \frac{H_0 f_0^2}{R\rho_0}\frac{\partial}{\partial z}\frac{\rho_0}{\Gamma}\frac{\partial}{\partial z}(\hat{U}y + \hat{\Psi}) + \frac{\hat{\beta}}{\hat{U}} \times (\hat{U}y + \hat{\Psi}) = 0, \tag{7.8}$$

where

$$\hat{\beta} \equiv \beta - \frac{H_0 f_0^2}{R\rho_0}\frac{\mathrm{d}}{\mathrm{d}z}\frac{\rho_0}{\Gamma}\frac{\mathrm{d}}{\mathrm{d}z}\hat{U}.$$

Although eq. (7.8) happens to be linear for our particular choice of upstream meridional shear, the total wave system is still fully nonlinear because of the lower boundary condition (3.6), which is

$$J\left[\hat{\Psi}, \left\{\frac{H_0 f_0}{R\Gamma}\hat{\Psi}_z + h\right\}\right] + \frac{H_0}{f_0}\frac{1}{\tau_E}\nabla^2\hat{\Psi} = (\hat{Q} - \hat{Q}^{(u)})/\Gamma - (\mathrm{TEH} - \mathrm{TEH}^{(u)}), \qquad \text{at } z = z_1. \tag{7.9}$$

In the more general case in which forcing due to topography and differential heating is not localized, there may not exist an "upstream" region for the atmosphere as we have assumed earlier. Periodicity along a zonal circle is the only boundary condition that can be imposed in the x-direction. It turns out that our solution to (7.8) is *also* a solution for this more general case if it is required to be periodic. The solution for that case should be interpreted as the solution to (7.7) which, if asymmetric forcing is absent, would possess a basic-state zonal flow (7.5) which is meridionally uniform.

7.2. *Solution procedure*

The topographic elevation of the earth's surface is taken from Scripps' 1° × 1° record (Gates and Nelson, 1975). The grid-point data are Fourier analyzed into the form of a double Fourier series:

$$h(x,y) = \mathrm{Re}\sum_{m=0}^{M}\sum_{n=0}^{N} h_{mn} e^{imx'} \sin ny', \qquad 0 \leqslant x' \leqslant 2\pi, \qquad 0 < y' < \pi, \tag{7.10}$$

where x' is x nondimensionalized by $a\cos\theta_0$ and y' is $y - y_1$ made dimensionless by $(y_2 - y_1)/\pi$. The solution $\hat{\Psi}$ is also expressed in a similar double Fourier series:

$$\hat{\Psi} = -\hat{U}\cdot(y - y_1) + \hat{\psi},$$

$$\hat{\psi} = \mathrm{Re}\sum_{m=0}^{M}\sum_{n=0}^{N} \phi_{mn} e^{imx'} \sin ny', \qquad 0 < y' < \pi. \tag{7.11}$$

[Note that despite the presence of an induced mean zonal flow by the $m = 0$ component of the nonlinear perturbation, the integral over the channel of the zonal flow is the same as that upstream, consistent with (2.6). However, because of this wave induced mean flow, $\bar{u}(y,z)$ is different from $U(z)$: the former is predicted while the latter is

prescribed.] The vertical structure equation for $\phi_{mn}(z)$ is found by substituting (7.11) into (7.8)

$$\frac{H_0 f_0^2}{R\rho_0}\frac{\mathrm{d}}{\mathrm{d}z}\frac{\rho_0}{\Gamma}\frac{\mathrm{d}}{\mathrm{d}z}\phi_{mn} + \left[\frac{\hat{\beta}}{\hat{U}-\left(\frac{m}{a\cos\theta_0}\right)^2-\left(\frac{\pi n}{y_2-y_1}\right)^2}\right]\phi_{mn}=0. \tag{7.12}$$

Eq. (7.12) is solved numerically using the Lindzen-Kuo up-down sweep for each wave number. The numerical domain is from the surface to 100 km divided into 100 to 900 levels (depending on the convergence of the solution). Near the top of the domain, $\hat{U}$ and Γ are assumed to be independent of z so that either the radiation or boundedless condition can be applied to the density-weighted solution in the following manner

$$\frac{\mathrm{d}}{\mathrm{d}z}\rho_0^{1/2}\phi_{mn} = i\left[\frac{R\Gamma}{H_0 f_0^2}\left(\frac{\beta}{\hat{U}}-\left(\frac{m}{a\cos\theta_0}\right)^2-\left(\frac{\pi n}{(y_2-y_1)}\right)^2\right)-\frac{1}{4H_0^2}\right]^{1/2}\rho^{1/2}\phi_{mn}$$

at the top,

where the square root is taken to be positive if the sum of the terms inside the brackets is positive. Otherwise, the positive imaginary root is taken.

For the case $\Delta T^* \equiv 0$, (7.12) can be solved analytically, yielding

$$\phi_{mn}(z) = A_{mn}\exp\left\{P_{mn}\frac{(z-z_1)}{H_0}\right\}, \tag{7.13}$$

where

$$P_{mn} = \tfrac{1}{2} + i\left\{\frac{RH_0\Gamma}{f_0^2}\left(\frac{\beta}{\hat{U}}-\frac{m^2}{a^2\cos^2\theta_0}-\frac{\pi^2 n^2}{(y_2-y_1)^2}\right)-\tfrac{1}{4}\right\}^{1/2} \tag{7.14}$$

For the more general case of $\Delta T^*(z)$, we define

$$P_{mn} \equiv H_0\left[\frac{\mathrm{d}}{\mathrm{d}z}\phi_{mn}(z_1)\right]/\phi_{mn}(z_1). \tag{7.15}$$

Its value is found numerically and stored.

Substituting (7.11), (7.10) and (7.15) into the lower boundary condition (7.9) yields a nonlinear equation for A_{mn} involving four-fold infinite sums. Two of them can be removed using the orthogonal condition of trogonometric functions. The result is

$$\sum_{\bar{m}=-M}^{M}\sum_{\bar{n}=-N}^{N}(m\bar{n}-\bar{m}n)A_{\bar{m}\bar{n}}\times\left[\frac{f_0}{R\Gamma}P^0_{m-\bar{m},n-\bar{n}}A_{m-\bar{m},n-\bar{n}}+h_{m-\bar{m},n-\bar{n}}\right]\times(\delta_{m,\bar{m}}+1)(\delta_{\bar{m},0}+1)$$
$$=(\delta_{m,0}+1)\left\{m\frac{4U_0(y_2-y_1)}{\pi}h_{mn}+\left[m\frac{4U_0(y_2-y_1)f_0}{\pi R\Gamma}\left(P^0_{mn}-\frac{H_0\hat{U}_z(z_1)}{U_0}\right)+4i\frac{H_0}{f_0\tau_E}\left(\mu m^2+\frac{1}{\mu}n^2\right)\right]A_{mn}-\frac{i4a\cos\theta_0(y_2-y_1)}{\pi}(\chi_{mn}-q_{mn})\right\}, \tag{7.16}$$

where

$\delta_{m,\bar{m}} = 1$ if $m = \bar{m}$ and 0 otherwise,

$P^0_{mn} = P_{mn}$ if $m \neq 0$, and $P^0_{0n} = \mathrm{Re}P_{0n}$

$$\mu \equiv \frac{(y_2-y_1)}{\pi a\cos\theta_0}$$

$\mathrm{Im}h_{0n} = 0$, $\mathrm{Im}A_{0n} = 0$,

$h_{-m,n}$ = complex conjugate of $h_{m,n}$

$h_{m,-n} = -h_{m,n}$

and similarly for A_{mn}. We have also written, at $z = z_1$

$$\mathrm{TEH} - \mathrm{TE}\hat{H}^{(u)} = \mathrm{Re}\sum_{m=0}^{M}\sum_{n=0}^{N}\chi_{mn}e^{imx'}\sin ny',$$

$$(\hat{Q}-\hat{Q}^{(u)})/\Gamma = \mathrm{Re}\sum_{m=0}^{M}\sum_{n=0}^{N}q_{mn}e^{imx'}\sin ny'.$$

Eq. (7.16) is to be solved numerically to determine the surface amplitude A_{mn}, given the topographic, diabatic and transient forcings: h_{mn}, q_{mn} and χ_{mn} respectively. This is done for each value of U_0. Thus the result is dependent on U_0 parametrically, i.e.

$$A_{mn} = A_{mn}(U_0).$$

For each value of U_0, we can also evaluate the mountain torque from

$$\mathcal{F}(U_0) = \frac{f_0}{H_0(y_2 - y_1)} \int_{y_1}^{y_2} \overline{\frac{\partial}{\partial x} \hat{\Psi}|_{z_1}} h dy$$

$$= \frac{f_0}{4a \cos\theta_0 H_0} \sum_{m=1}^{M} \sum_{n=1}^{N} \mathrm{Im}\{mh_{mn} \cdot \text{complx. conj } (A_{mn}(U_0))\}. \quad (7.17)$$

The result (7.17), when substituted into the equation for the zonal index

$$\frac{\partial}{\partial t} U_0 = \frac{1}{\tau_E} (U^* - U_0) + \mathcal{F}(U_0), \quad (7.18)$$

then completes the formulation for the evolution equation. If

$$U_0 = U_0(t)$$

is found as a solution to eq. (7.18), the time dependent evolution of the stationary waves is determined through their parametric dependence on $U_0(t)$, i.e.

$$\hat{\Psi} = \hat{\Psi}(U_0(t)).$$

The numerical procedure for solving (7.16) is Newton's method with arc-length continuation, and is described in more detail by Rheinboldt and Burkardt (1983a, b). The upper limits of spectral truncation, M and N, are chosen so that a further increase in resolution will not change the numerical results noticeably. Typical values of M and N for convergence are $M = 15$ and $N = 4$ to 8. However, we have not performed calculations with resolutions beyond $M = 30$ and $N = 8$.

7.3. *Results for the case of* $\Delta T^* \equiv 0$

In this set of calculations, the channel width is taken to be 33 degrees of latitude from $\theta_1 = 30°$ N to $\theta_2 = 63°$ N. Although a wider channel appears to be more consistent with our lateral channel boundary condition of vanishing normal velocity for the stationary wave, the present choice of channel width is the same as that of Charney and Eliassen (1949) and Charney et al. (1981), and so allows easier comparison of our results with theirs.

The reference case: In the reference case, topography constitutes the only form of surface forcing for the stationary waves. Surface differential heating and transient eddy flux forcings are neglected.

Calculations are made for a number of Ekman damping time scales. A reference value is given by

$$\tau_E \simeq 5.7 \text{ days},$$

corresponding to a bulk eddy viscosity coefficient of $\nu_E \simeq 5$ m^2/s, a value adopted previously by Charney and Eliassen (1949). Calculations are also performed using

$$\tau_E \simeq 14.3 \text{ days},$$

a value adopted (implicitly) by Charney et al. (1981).

In Fig. 5 the mountain torque term, $-\mathcal{F}(U)$, is plotted as a function of U for $\tau_E = 5.7$ days (the symbol $\hat{U}$ is replaced by U for convenience). The dashed and solid curves show the quasi-linear (obtained by neglecting the left-hand side of (7.16)) and nonlinear solution respectively, and the solid straight lines show $\tau_E^{-1}(U^* - U)$. The intersections of the straight lines with the curves give the equilibrium points. The intersections of the straight with the U-axis give the values of U^*. It is evident from the figure that, no matter what value of U^* we

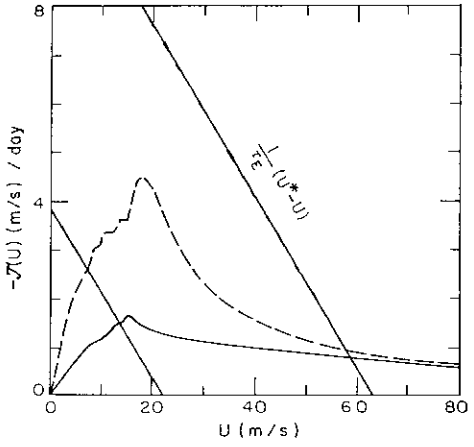

Fig. 5. Mountain torque $-\mathcal{F}(U)$ as a function of U, for the reference case of topographic forcing only and $\tau_E = 5.7$ days. The solid curve refers to the nonlinear solution. The dashed curve represents the linear solution obtained by dropping the left-hand side of Eq. 7.16. The straight lines show $\tau_E^{-1}(U^* - U)$ versus U for $U^* = 22$ and 63 m/s. The intersection of each line with the horizontal axis shows the value of U^* used for that line. The intersections of the straight lines with the mountain torque curves give the equilibrium values of U.

use, *there are no multiple equilibria for the nonlinear solution*, in spite of the fact that for some values of U^* the truncated (quasi-linear) solution permits 3 equilibria as in Charney and DeVore (1979).

When a longer damping time of $\tau_E \simeq 14.3$ days is used, resonance of individual wavenumbers becomes more prominent in the linear solution, as shown in Fig. 6. Multiple equilibria are present for the *quasi-linear* solution with $U^* \simeq 63$ m/s, in almost identical fashion as found by Charney et al. (1981). The mountain torque calculated using the converged nonlinear solution is however drastically different from the truncated case. Fig. 6 shows that the magnitude of the nonlinear mountain torque is about a factor of 3 to 6 smaller than that calculated using the quasi-linear solution. This is due mainly to the fact that the interaction between the wave and *mean shear* is neglected in the quasi-linear solution. This interaction, which is incorporated in the nonlinear solution, is responsible for transferring a significant portion of the wave energy into the $m = 0$ modes, which do not produce any mountain torque.

Generally there is only one equilibrium found for the nonlinear solution, except for a narrow range of U^* around 32 m/s where there is some indication of three equilibria (two stable and one unstable) for the present case of $\tau_E \simeq 14.3$ days. We attribute the presence of the multiple equilibria in this case to the fact that at the large values of U for which these equilibria are found, forcing due to flow over mountain, represented by the term $U\partial h/\partial x$, is substantially higher than is the case for the real atmosphere where U near the surface is around 2 to 3 m/s. This problem, caused by our neglect in this set of calculations of the substantial vertical shear found in the lower atmosphere, is common to both the $\tau_E = 5.7$ day case and the 14.3 day case. However, in the second case, the smaller damping in the system magnifies the effect of the unrealistically large forcing. In Figs. 7 and 8 we show the equilibrium stationary wave field solution calculated for $\tau_E = 5.7$ days and 14.3 days, respectively. We see that the case with the longer damping time appears to overestimate the observed climatological amplitude of Oort (1983). This is true especially for the linear solution and is perhaps a reason why the multiple equilibria are more prominent for the quasi-linear case at $\tau_E = 14.3$ days (see Fig. 6).

The problem of too much forcing by the flow over mountain term is a common feature for barotropic models. The usual remedy is to adopt the "equivalent barotropic" assumption of Charney and Eliassen (1949). This involves multiplying the U in the flow over mountain term, $U\partial h/\partial x$, by a factor $\kappa \simeq 0.4$, to empirically account for the ratio of the

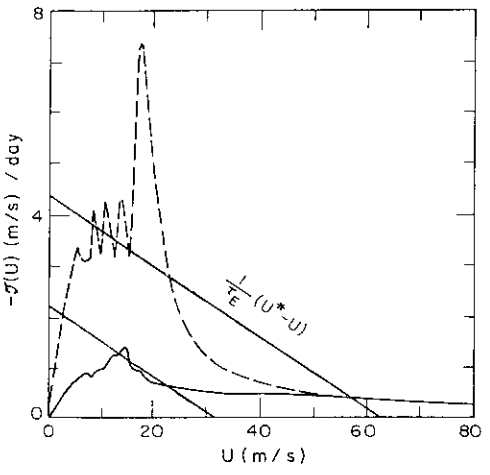

Fig. 6. Same as in Fig. 5, except for $\tau_E = 14.3$ days. The straight lines show τ_E^{-1} $(U^* - U)$ for $U^* = 32$ and 63 m/s.

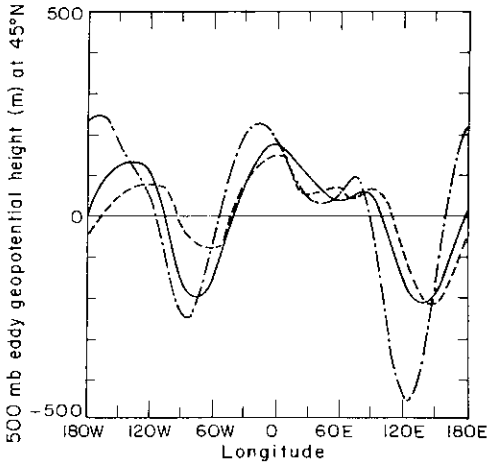

Fig. 7. 500 mb stationary wave geopotential height as a function of longitude at 45 ° N for the reference case with $\tau_E = 5.7$ days and $U = 14$ m/s. The solid curve shows the non-linear solution, the curve with long dashes shows the linear solution, and the curve with short dashes shows the observed winter climatological mean (Oort, 1983).

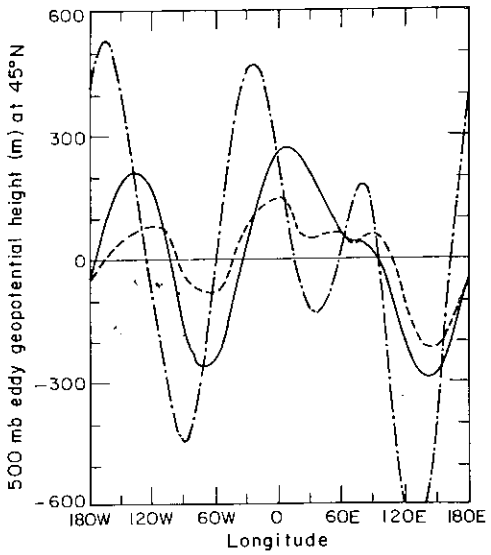

Fig. 8. Same as in Fig. 7 except for $\tau_E = 14.3$ days.

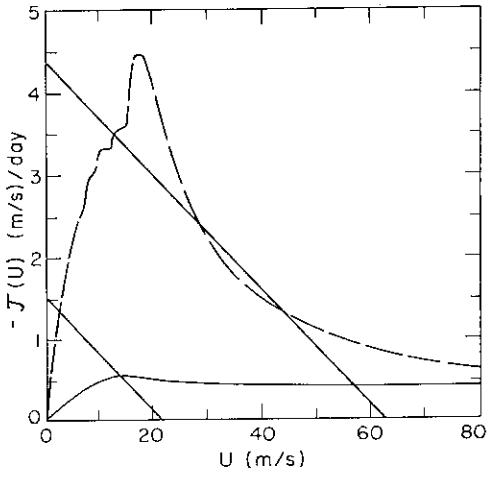

Fig. 9. Mountain torque $-\mathcal{J}(U)$ versus U. The notation is the same as in Fig. 5, except now $\tau_E = 14.3$ days and solutions have been calculated by multiplying the U in the flow over mountain term by the factor $\kappa = 0.4$.

surface U to the U at the "equivalent barotropic" level. Although we believe that the effect of vertical shear should be more consistently accounted for in a 3-D model that explicitly takes it into account, as we will discuss in a moment, for comparison we have repeated the calculation for the $\tau_E = 14.3$

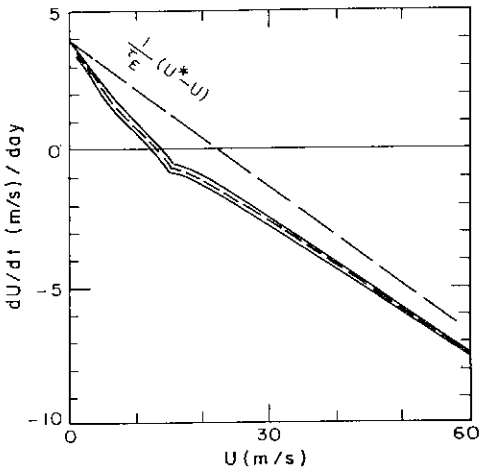

Fig. 10. Phase diagram of dU/dt versus U for nonlinear solutions calculated with $\tau_E = 5.7$ days. The reference case calculated without transient eddies (but with topographic forcing only) is shown by the top solid curve. The middle dashed curve is calculated using transient eddy heat fluxes with χ_{mn} having the observed amplitude (Lau, 1979). The bottom solid curve is calculated with twice the observed transient heat flux. The dashed straight line shows dU/dt in the absence of mountain torque.

days case with the flow over mountain term scaled by κ. The result for the mountain torque is shown in Fig. 9. The situation is similar to that in Fig. 5. *Only one equilibrium* is found for any value of U^*. The stationary wave amplitudes (not shown) are closer to the observed than in the case without the scaling factor.

7.4. Effect of transient eddy flux convergence

The stationary wave solution presented in section 7.3 is calculated without taking into account the transient eddy heat flux term, χ_{mn}, in the lower boundary condition (7.16). The calculation is repeated here with χ_{mn} prescribed according to the observational analysis of Lau (1979), who gave a table of the Fourier coefficients of TEH for $m = 1$ to 4 at 40° N, 50° N and 60° N. Our χ_{mn}'s are calculated using these data for the first 4 wavenumbers; the rest of the Fourier coefficients are taken to be zero.

It should be noted that the transient eddy fluxes in Lau (1979) were climatological seasonal averages. Monthly averages would have been more appropriate for our purpose but these are not

available in a convenient form. There is some indication, judged by the contour maps presented in Lau (1984), that the monthly average heat fluxes are of comparable amplitude and approximate phase as the seasonal averages. Thus it appears reasonable to assume that since $t_T \sim 1$ month is sufficiently long for the purpose of obtaining stable transient eddy statistics, that such statistics probably will not change sufficiently when t_T is increased to a season (provided the (predictable) seasonal cycle is removed). To take some account of the variance from climatology, we have repeated the calculation with the magnitudes of the χ_{mn}'s increased by a factor of two from those given by Lau.

In Fig. 10, the phase diagrams for the zonal index calculated using the fully nonlinear stationary wave solution with and without *prescribed* χ_{mn} are depicted. In Fig. 11, we show the stationary wave amplitudes with and without the prescribed transient eddy heat fluxes. The impression given by these two figures is as follows: Although the transient eddy fluxes can have some effect on the wave *amplitude* (namely, increasing the Pacific and Alantic ridges, presumably due to the storm tracks in these regions), and also can contribute to some *variability* of the stationary waves (by altering slightly the slope of the phase diagram), the situation is still *predictable* according to our criterion discussed in Section 5, provided that the transient eddy fluxes can somehow be *prescribed* to be not too much larger than a few times the climatological seasonal mean values given by Lau (1979). Note that this conclusion is based on the $\Delta T^* \equiv 0$ case; results will be somewhat different when a more realistic $\Delta T^*(z)$ is used, as will be discussed in Subsection 7.6.

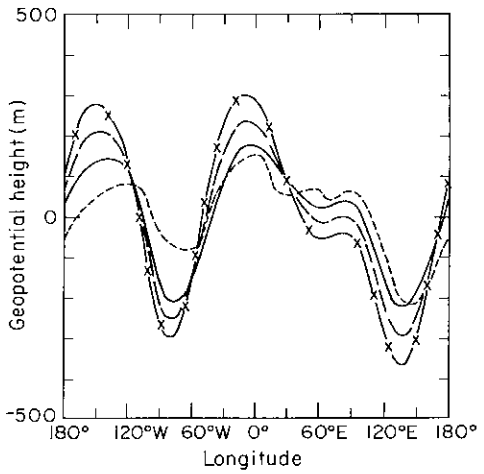

Fig. 11. 500 mb stationary wave geopotential height as a function of longitude at 45° N when $\tau_E = 5.7$ days and $U = 14$ m/s. The solid curve shows the nonlinear solution found without transient eddies (but with only topographic forcing); the curve with long dashes is obtained with χ_{mn} found from the observed amplitude of transient eddy flux (Lau, 1979); and the solid curve marked with crosses is obtained with twice the observed transient heat flux. The curve with short dashes shows the observed winter climatological mean (Oort, 1983).

7.5. *Results for realistic* $\Delta T^*(z)$

For the following set of runs, the channel boundaries, θ_1 and θ_2, are placed at 30° N and 90° N, respectively. Calculations have also been performed with a 33 degree channel as in Subsection 7.3, with results similar to those for the 60-degree channel case as far as the evolution of the zonal index is concerned. The damping time used in the majority of the calculations is taken to be $\tau_E = 5.7$ days, corresponding to a commonly adopted value for bulk eddy viscosity of $\nu_E \simeq 5$ m^2/s. The temperature difference

$$\Delta T^*(z) \equiv \hat{\bar{T}}(y_1, z) - \hat{\bar{T}}(y_2, z)$$

is prescribed to be consistent with the observed Northern Hemisphere wintertime climatology. Specifically, we have specified the channel averaged vertical shear, $\hat{U}_z$, which is proportional to ΔT^*, according to the thermal wind relation (4.13). This quantity is computed for convenience using the analytic formula given by eq. (38) in the paper by Tung and Lindzen (1979b), which conveniently gives a good approximation to the observed $\hat{U}$.

It should be noted that even though the temperature difference ΔT^* between the two channel boundaries is prescribed, the actual temperature distribution $\hat{T}(x, y, z)$ and its zonal mean $\bar{\hat{T}}(y, z)$, are not. These latter quantities are free to respond to stationary waves through wave-mean flow interaction. In particular $\hat{\bar{T}}(y, z)$ is predicted in the present model as part of the solution. Thus the response of the model should be considered as baroclinic.

To illustrate this point, we show in Fig. 12 *calculated* distributions of the zonal mean flow $\hat{u}(y, z)$ for both the 33°- and 60°-channels and for selected values of $U_0(t) \equiv \hat{U}(z_1, t)$ as indicated in

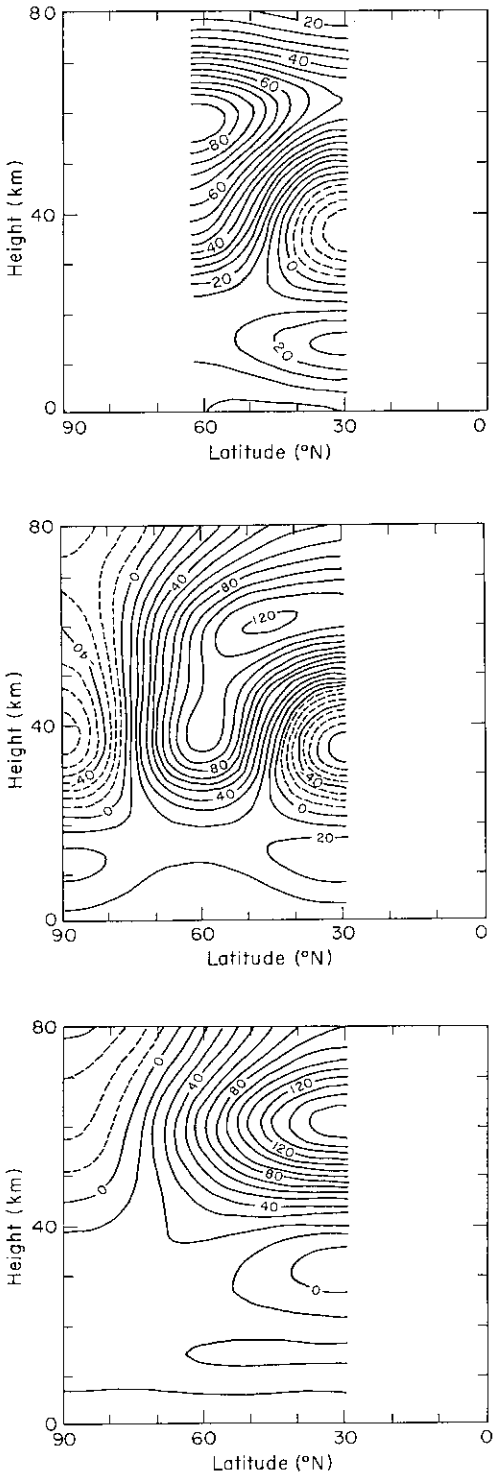

the legend. Note that the presence of meridional shears shown is due entirely to the mechanism of topographic wave-mean flow interaction as far as these calculations are concerned. In this mechanistic model with the simplifying assumptions described earlier in this section, there should be no meridional shear when the zonally asymmetric stationary forcing (due to topography) is removed. The mean zonal wind in that case is then

$$\hat{u} = \hat{U}(z)$$

with no y-dependence. This can be considered as our zonally symmetric basic state (sometimes referred to as a "radiative equilibrium" state). With the mountain forcing "switched on", zonal asymmetries develop and these induce both meridional and vertical shears in the mean zonal wind. Even for the narrow channel case shown in Fig. 12a, the induced shears are realistic enough to produce a tropospheric jet near tropical latitudes with 25 m/s speed, a stratospheric jet of 85 m/s with its axis located near mid to high latitudes and slanting poleward and downward, and an intrusion of the summer hemisphere easterlies into the winter hemisphere above the tropospheric jet maximum. These features are described by, for example, Holton (1972), as typical of the observed wintertime climatology. For the wider channel case, the zonal wind distribution is less constrained and can evolve into a larger number of configurations depending on the input parameters U_0 and ΔT^*. In Fig. 12b, we show a case with $U_0 = 3$ m/s, where the stratospheric jet maximum is moved equatorward and has a greater maximum speed of 120 m/s. To maintain the same cross-channel temperature difference, easterlies are produced over the pole in the stratosphere. The tropospheric jet stays at approximately the same location but with a slightly reduced speed of 20 m/s.

An indication of the variability of the calculated mean zonal wind can be obtained by comparing Fig. 12b with 12c. The latter is calculated using a U_0 which is 30% larger. Consistent with the higher value of westerly momentum influx, Fig. 12c shows

Fig. 12. (a): Distribution of the zonal mean wind $\bar{u}(y,z)$ calculated from the non-linear solution in a 33° channel with $\tau_E = 5.7$ days and the same $\hat{U}_z$ as used by Tung and Lindzen (1979b), with $U_0 = 3.9$ m/s. (b): Same as in (a), except for a 60° channel with $U_0 = 3$ m/s. (c): Same as in (b), except for $U_0 = 3.9$ m/s.

a diminished easterly intrusion from the summer hemisphere, a broader tropospheric westerly jet, and the disappearance from the stratosphere of the easterly region over the pole. The stratospheric jet maximum is shifted equatorward, with its large winds mostly confined to the mesosphere.

In Fig. 13, we compare our calculated wave geopotential height with the observed stationary-wave geopotential height derived from 11 years of NMC operational analyses by Lau (1979) (see Wallace (1983)). In Fig. 13a, the observed longitude-height cross-sections at 45° N are displayed. In Fig. 13b, the calculated cross-sections are displayed for a case corresponding to conditions imposed for Fig. 12c (with $U_0 = 3.9$ m/s). In Fig. 13c, the case is the same as Fig. 13b, except for $U_0 = 3$ m/s (corresponding to Fig. 12b)

Generally, stationary wave solutions have a larger zonal wavenumber character below 30 km than above, consistent with existing theories of wave propagation (Charney and Drazin, 1961; Matsuno, 1970; Tung and Lindzen, 1979b). Amplitudes in the stratosphere and mesosphere are very variable (more precisely, more sensitive to U_0 and ΔT^*), consistent with the observation of Geller et al. (1984). In the lower atmosphere, where density is higher, calculated variability is not as large as above, but nevertheless our solution still displays non-negligible variation from case to case. This behavior shows more variability and sensitivity than found by Jacqmin and Lindzen (1985).

Focusing our attention to heights below the 100 mb level, where data in Fig. 13a are available, we shall compare our calculated amplitude and phase with the observed climatology. In general, the agreement between Fig. 13b and 13a is excellent. However, given the variability from case to case, the agreement should perhaps be regarded as fortuitous. We will comment on this point later. Referring to the highs and lows by their surface locations, following common practice, we find a shallow Siberian High, an Aleutian Low with a strong westward tilt with height and a 300 meter maximum aloft, an Eastern Pacific/Western North America High of 150 meters in the lower stratosphere, a weak southern extension of the Icelandic Low of 60 meters amplitude, and finally a more intense Eastern Atlantic High of more than 150 meters aloft. These calculated features and their longitudinal and height locations are strikingly close to the observed climatology in 13a.

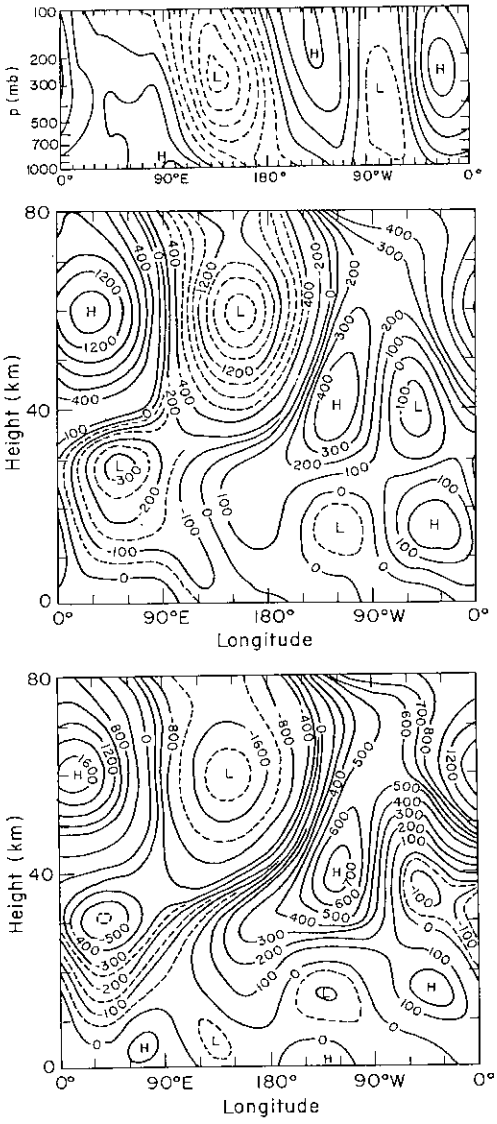

Fig. 13. Longitude-height cross section at 45° N of stationary-wave geopotential height (a): derived from 11 years of NMC operational analyses by Lau (1979). (The contour interval is 50 m and the zero contour is thickened); (b): calculated for a case corresponding to conditions imposed for Fig. 12c (with $U_0 = 3.9$ m/s); (c) calculated for a case corresponding to conditions imposed for Fig. 12b (with $U_0 = 3$ m/s).

With a lower momentum budget for the channel ($U_0 = 3$ m/s), Fig. 13c has some noticeable discrepancies from the observed climatology. The number of surface highs and lows remain the same,

but the lows are tilting more steeply with height (due probably to our ΔT^*, which is prescribed to be somewhat weaker than the climatology at the tropospheric jet maximum level). Consequently the low Aleutian center aloft is now situated above the Siberian High. Similarly, the westward tilt of the Icelandic Low displaces the North American High aloft to a more western location than observed. Also the amplitude near the surface is generally smaller than observed, and smaller than the previous case of $U_0 = 3.9$ m/s, which has a 30% more net flow over the topography.

It should be mentioned again that these calculations are performed using topography as the only form of forcing. Differential heating, which should also be important in forcing the stationary waves in the lower atmosphere, has been ignored. In view of the variability inherently present in the topographically forced stationary wave solutions and the sensitivity of the solution to different mean budget parameters, perhaps one should not use the good agreement we have obtained with observation under a set of conditions using only topographic forcing to conclude that diabatic heating is not as important as topography as a forcing mechanism for stationary waves.

The present purpose of comparing our result with observation is simply to show that our model solution is of *comparable* amplitude and phase as observed, thus lending some credibility to our choice of parameters (e.g. τ_E, U^* and ΔT^*). What is more important from the present standpoint is the phase diagram in Fig. 14, produced under what we now claim to be *realistic* conditions. It shows only one "equilibrium" for a realistic range of values of zonal momentum driving U^*. Three equilibria are found only for $U^* \sim 25$ m/s, an unrealistically large value which cannot be physically justified by the lateral flux of angular momentum from the tropics.

Based on these simple calculations, we tentatively conclude that internal nonlinear interactions among the large-scale waves are not likely to lead to unpredictability of the extratropical large-scale flows. We further suggest that it is not necessary to attribute some of the observed low-frequency variability to internal transitions between multiple equilibria (cf. Charney and DeVore, 1979; Charney et al., 1981). Considerable variability can be induced by the variability of the external forcing parameters. Comparison of Fig. 13b with Fig. 13c shows the variability that can be induced by the variability in $U^*(t)$ arising from transient momentum flux from the tropics. (A variability in U^* induces variability in the "equilibrated" value of the surface zonal index U_0. A change in U_0 yields different stationary wave responses, as shown in Fig. 13b and c.)

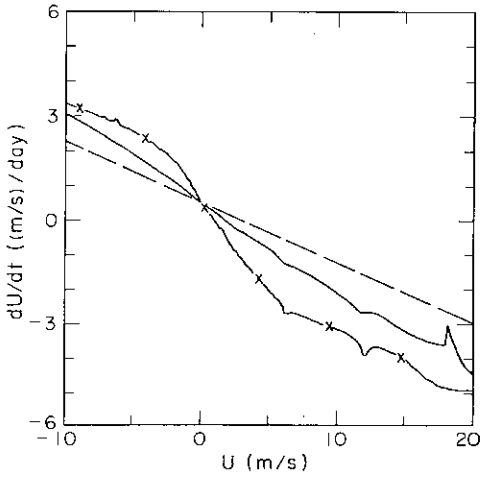

Fig. 14. Phase diagram of dU/dt versus U calculated for $\tau_E = 5.7$ days, $U^* = 3$ m/s, a 60° channel, and the same $\hat{U}_t$ as used by Tung and Lindzen (1979b). The solid curve shows the nonlinear solution and the solid curve marked with crosses shows the linear solution. The dashed straight line shows dU/dt in the absence of mountain torque.

Another mechanism for inducing variability of the extratropical flow is through the tropical heat flux, which changes the heat budget in the extra-tropics (in particular, it changes ΔT^*). We simulate this variability with our model by changing ΔT^* slightly. In particular we reduce ΔT^* at the stratospheric jet maximum level (~ 60 km) by 20% (by changing the value of U_2 in eq. (38) of Tung and Lindzen (1979b) from 150 m/s to 120 m/s). This is within the range of month-to-month variability Geller et al. (1984) reported for the real atmosphere. The resulting solution is shown in Fig. 15. Comparing the calculated mean zonal wind distribution in 15a with that in 13b, we see that a lowered value for the zonal index at the 60 km level leads to a lower speed for the stratospheric jet stream maximum. The easterlies over the pole are replaced by a secondary westerly jet centered around the 40 km level. The easterly

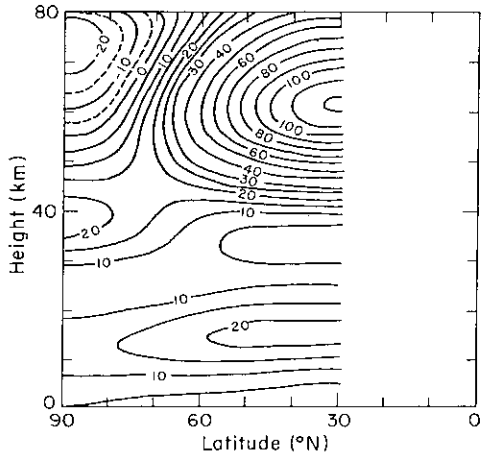

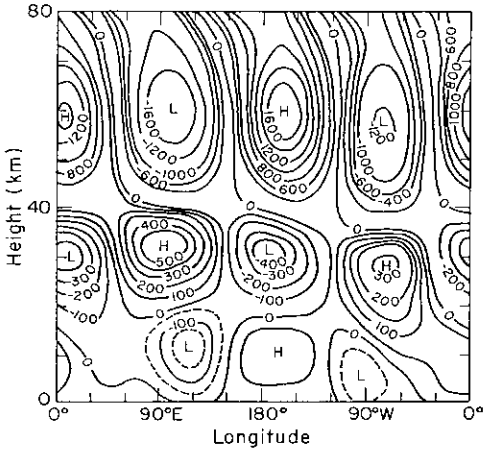

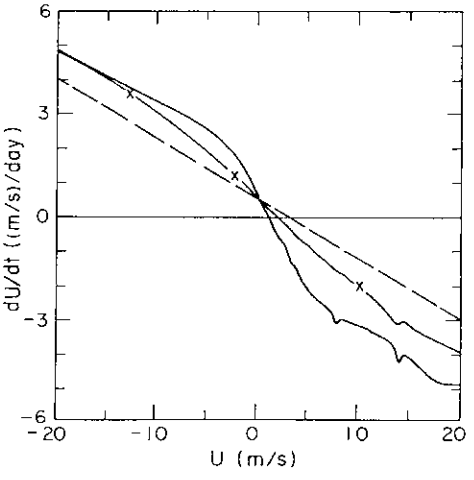

intrusion from the summer hemisphere now becomes much weaker. The tropospheric jet becomes broader with a much reduced meridional shear throughout the channel. Comparing the wave geopotential height distribution in Fig. 15b with that in Fig. 13c, we see that the reduced stratospheric jet speed allows shorter wavelengths to penetrate to the upper atmosphere (Above 40 km, Fig. 13c is dominated by a wavenumber 1 disturbance, while Fig. 15b is predominantly wavenumber 2.) The vertical distribution of the wave solution in Fig. 15b is also more baroclinic (with shorter vertical wavelengths) than that depicted in 13c. The surface amplitudes (in particular the lows) are somewhat larger in 15b than 13c.

Despite these differences induced by variability in the heat budget, the phase diagram displayed in Fig. 15c shows a strong resemblance to that in Fig. 14. In particular, both show what we regard as predictable behavior, as far as our model is concerned.

7.6. Interaction between the low- and high frequencies

To assess the effect of transient eddy flux on the predictability and variability of the low-frequencies in a realistic baroclinic model, we apply the procedure used before in Subsection 7.4 for the "barotropic" model to the present case of realistic vertical shears. The observed climatological transient eddy heat flux of Lau (1979) is expanded in a Fourier series as before except now for a 60° channel (instead of 33° as in Subsection 7.4). The coefficients χ_{mn} thus calculated are used in (7.16) to calculate the stationary wave amplitudes. The resulting phase diagrams are shown in Fig. 16.

Without the transient eddy heat fluxes, the phase diagram is the same as that in Fig. 14, as the applicable conditions are otherwise the same for both figures. With the climatological values of the transient eddy fluxes incorporated, the phase diagram shows the same predictability quality as

Fig. 15. (a): Distribution of the zonal mean wind for the same case as in Fig. 12b, except that ΔT^* at the stratospheric jet maximum level has been reduced by 20%. (b): Longitude height cross section at 45° N of wave geopotential height calculated for the same case as in (a). (c): Phase diagram of dU/dt versus U for the same case as in Fig. 14, except that ΔT^* at the stratospheric jet maximum level has been reduced by 20%.

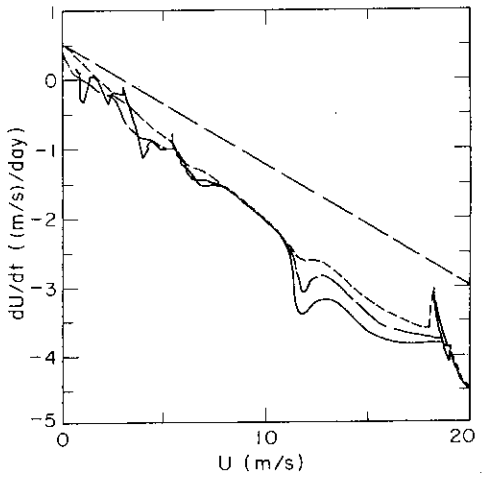

Fig. 16. Phase diagram of dU/dt versus U. The curve with short dashes shows the nonlinear solution for the same case as in Fig. 14 (without transient eddy heat fluxes); the curve with long dashes shows the solution when χ_{mn} has values inferred from the observed climatological transient eddy heat flux (Lau, 1979); and the solid curve shows the solution calculated using twice these values. $U^* = 3$ m/s. The abscissa should be shifted for other values of U^*.

the case without the transient eddies. Namely, the system is predictable except for an unrealistically large value of $U^*(\sim 25$ m/s) which cannot be physically justified by the lateral flux of angular momentum from the tropics.

However, unlike the "barotropic" case, which does not show much sensitivity to a doubling of the magnitudes of the transient eddy fluxes from their climatological values, the present baroclinic model shows the emergence of multiple equilibria for some (realistic) values of U^* when we double the magnitudes of χ_{mn} from their values calculated from Lau's (1979) climatological data. [*Note added in proof.* The sensitivity to thermal forcing (due to transient eddies in this case), found for the baroclinic atmosphere may have been amplified by the absence of thermal damping in the present model. We further found that such a sensitivity can cause complicated fine structures in both of the lower two curves in Fig. 16 when the increment in the continuation parameter U is reduced to lie between 10^{-4} and 0.1 m/s. These fine structures are not shown in Fig. 16, which was obtained with a permitted maximum increment of 0.2 m/s in U.]

Physical interpretations of this model result are somewhat problematic, especially concerning the predictability issue, because our transient eddies are not interactively calculated. On the other hand, our procedure of prescribing the transient eddy fluxes from observation probably does not suffer as much the drawbacks of some models that predict too much transient eddy activity when compared to the real atmosphere (see Subsection 7.7). Concerning the predictability of the real atmospheric flows, it appears that one can infer the following preliminary results from our present calculation.

(i) While the effect of transient eddies is significant, the evolution of the stationary waves is not dominated by the interaction between high and low frequencies (cf. Reinhold and Pierrehumbert (1982)). In fact, our model result suggests potential extended-range predictability if the transient eddy fluxes are close to the climatological value of Lau (1979).

(ii) Nevertheless, if the *uncertainty* in our knowledge of the transient eddy fluxes is as large as the climatological values of these eddy fluxes, unpredictability of the low frequencies can result according to the criterion put forth in Subsection 5.2

(iii) Assuming that the fluctuation of the transient eddy statistics becomes larger with shorter averaging periods t_T, one can probably infer from the present calculations that the low frequency flows in our atmosphere are probably near the borderline of predictability or unpredictability under certain conditions involving the vertical shears, when the averaging period is less than a month. Thus it appears that while extended-range prediction of the seasonal and monthly means may be potentially possible, it is not clear at present if the long-range forecast of the weekly means is feasible.

7.7. *Comparison with previous two-layer model results*

There appear to be some significant differences between the behavior of the solutions reported here and that obtained by other authors based on two-layer models. For example, Charney and Straus (1980) and Roads (1980) found 3 or even 5 equilibria in their two-layer models for each mode of topographic forcing, in the absence of synoptic

scale waves, while we find only one equilibrium even for a sum of many modes of topography. Reinhold and Pierrehumbert (1982) found that the transient baroclinic waves play a predominant role in affecting the evolution of large-scale topographically forced waves. In fact, they found that the presence of one additional zonal wave number in the unforced synoptic scale wave causes the evolution of the forced large-scale waves to be entirely different from that in the absence of this unstable synoptic wave as in the model of Charney and Straus. Seemingly chaotic and unpredictable behavior is found by Reinhold and Pierrehumbert.

Despite some fundamental differences in the formulation of the models quoted above and our present model (e.g. our baroclinicity is imposed by a prescribed cross-channel temperature difference ΔT^*, while theirs is forced by an internal "radiative" heat source $\Delta\theta^*$) many of the differences in model results can be qualitatively reconciled as due to differences in model parameters.

The first difference, as mentioned previously in this paper, is that all three two-layer models quoted above are channel models with *rigid* channel boundary conditions. Consequently the zonal momentum driving term U^* is absent in their models, with major consequences. Without a momentum source, which in the real atmosphere is provided by fluxes of momentum from the tropics, these models cannot maintain a *net* westerly flow in the lower layer of the model. Although it is conceivable that (even with a zero net momentum) westerlies in some latitudes and easterlies in others can be produced, it turns out that these two-layer models produce no zonal flow in the lower layer in the parameter range where the cross-channel difference in the "radiative equilibrium" temperature is between 0 °K and 69 °K for a channel width of 5000 km. Since no flow in the lower layer implies no topographic forcing even in the presence of topography, a zonally symmetric flow field results. This is the so-called "Hadley regime". It has only a upper level zonal flow forced by the temperature difference.

Had a momentum driving been introduced, as we have done with our U^* to represent the northward flux of westerly momentum that is present in the real atmosphere around 30° N, there would have been a flow over mountains in the lower layer and a wavy equilibrium could have obtained, as Källén (1983) showed with his two-layer model and as we have demonstrated with our three-dimensional model (see Subsection 7.5).

Wavy equilibria can be found in Charney-Straus type models only for large baroclinicity. When the cross-channel difference in the "radiative equilibrium" temperature exceeds 69 °K, the "Hadley flow" becomes unstable. Surface flows produced by instability interact with topography to produce 3 wavy equilibria when the aforementioned temperature difference is between 69 °K and 96 °K. Beyond 96 °K, 5 equilibria are found (for a one-mode topography). It is in this last parameter regime Charney and Straus (1980) obtained low index (blocking) and high index (zonal) equilibria, and it is in this highly baroclinic regime where Reinhold and Pierrehumbert (1982) studied the effect of allowing an unstable unforced baroclinic wave to develop without any momentum forcing for the stationary waves. Not surprisingly, Reinhold and Pierrehumbert found that all equilibria in the Charney-Straus model are highly baroclinically unstable, and that the effect of the transient wave is of extreme importance. As first pointed out by Rambaldi (1982), more realistic, and less unstable equilibria can be found if we restrict ourselves to a more realistic parameter regime (with a direct momentum forcing). It therefore appears that the "weather regime" diagram produced by Reinhold and Pierrehumbert, in which the trajectories of the forced large-scale wave are severely affected by the introduction of a baroclinically unstable synoptic wave, may be the result of adopting a large baroclinicity parameter for their model while the stationary waves are underforced. There is some indication that the effect of transients, while not negligible, may have been greatly exaggerated by their choice of parameters.

A second artifact of the two-layer models concerns the (again unrealistically) large interfacial friction term that has been adopted by Charney and Straus (1980) and Reinhold and Pierrehumbert (1982). This term is parameterized to be proportional to the difference of the zonal winds in the upper and lower layers of the model, and acts to transport zonal momentum from the top layer to the bottom layer through the interface. This vertical transport of momentum further increases the baroclinicity of the model. (This helps to explain the westward tilt of the wavy equilibrium solution in the Charney-Straus model in the presence of a

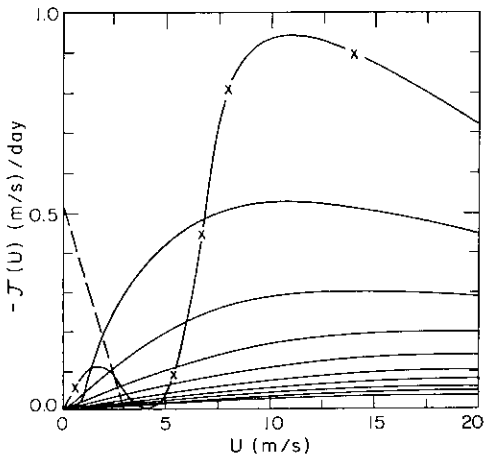

Fig. 17. Mountain torque $-\mathcal{T}$ (U) versus U for nonlinear solutions forced by a single-mode topography with $h_{2,1} = 600$ m in a channel from 30° N to 63° N with $\tau_E = 5.7$ days. The curve with crosses is for the case with $\hat{U}_z$ a constant determined from the thermal wind relation with $\Delta T^* = 10$ °C. The other solid curves are, from top to bottom, for cases with $\Delta T^* = 20$, 30, 40, ..., and 100 °C. The dashed line shows $1/\tau_E(U^* - U)$ for $U^* = 3$ m/s.

rigid lid). Källén (1983) has found that when this interfacial friction term is removed, only one equilibrium is found *no matter what the radiative equilibrium temperature difference is.*

In Fig. 17, we present the result from our third experiment, in which ΔT^* is prescribed to be a constant taking on values ranging from 0 °K to 100 °K. We see that, consistent with the finding of Källén, there is only one equilibrium for all values of ΔT^*. Also when U^* is zero as in the models mentioned above, this single equilibrium is the so-called Hadley flow (with no mountain torque). A wavy equilibrium is produced only when U^* is nonzero.

8. Conclusions

The aim of this article is to provide some theoretical basis to support the notion that large-scale quasi-stationary waves perhaps have extended range predictability. Through a scale analysis, it is shown, in Section 3, that the predictability of the running time mean of the large-scale *waves* is intimately related to the predictability of the *zonal index.* After showing, in the second half of this paper, that the zonal index is predictable under conditions to be summarized below, we suggest that the large-scale quasi-geostrophic waves may have the same predictability. More specifically,

(i) *Object to be predicted*: Low-frequency variability of the extra-tropical large-scale wave patterns and the associated zonal mean flow. The low-frequency portion is obtained by running time averaging. The length of time averaging is dictated by the requirement that the transient eddy statistics be stable (i.e. not highly variable) when averaged over a suitably long period.

(ii) *Range of prediction*: Longer than 10 days, with the upper limit determined by the range within which boundary forcings can be assumed to be prescribable. Detailed variability on the synoptic time scale is masked by the running time mean adopted in the definition of the quasi-stationary waves and so is not predicted.

(iii) *Effect of internal nonlinear dynamics on predictability*: This is studied in a mid-latitude channel model, in which the transient eddy flux is fixed, and radiative heating and lower boundary forcings are prescribed, but fully nonlinear large-scale wave-wave and wave-mean interactions are allowed. We find that the mechanism of wave-wave and wave-mean flow interaction for the quasi-stationary waves does not by itself lead to the unpredictability of the low frequencies.

(iv) *Effect of baroclinic transient eddies on predictability*: Conceding that the baroclinically unstable high frequencies are unpredictable at extended ranges, we examine only the predictability of the low frequencies. The question is, how severely are the low frequencies affected by the high frequencies. Our preliminary sensitivity assessments suggest that although the transient eddy fluxes can induce some low frequency variability through wave-wave interactions between the synoptic and planetary scales, such variability is likely to have some predictability beyond the "predictability limit". Nevertheless, we also find that if our uncertainty of the transient eddy statistics is large enough, unpredictability of the low frequencies can result. We should emphasize, however, that our result

on this point is far from conclusive, as our transient eddy fluxes are prescribed instead of internally generated in a fully time dependent model, and that more study is needed before this issue can be settled.

(v) *Effect of tropical influence on predictability*: Since the present model is not coupled interactively to a tropical atmosphere–ocean model, the present study cannot adequately assess the effect of tropical influence on the predictability of extra-tropical systems. Nevertheless, the rôle played by the tropics is isolated. First, the momentum flux from tropical disturbances can change the zonal momentum driving for the zonal index in the extra-tropical atmosphere, thereby altering the "equilibrium" value and the persistence of the stationary patterns. Second the upward and northward flux of heat from the tropics and the Hadley circulation can change the vertical shear of the zonal index, which in turn affects the vertical propagation and amplitude response of the large-scale waves in the extra-tropical region. Such induced variability, however, is still found to be predictable if the tropical influence can be *prescribed* as a lateral boundary forcing. Whether or not the combined system has extended-range predictability appears to depend on whether the coupling between the tropics and extra-tropics is linear or nonlinear in nature, and on whether or not the tropics are more predictable. Shukla (1984) has reviewed some evidence that tentatively suggests that at extended ranges, time and spacial means in the tropics may be potentially more predictable than in the extratropics.

In the present formulation, the predictability of the stationary long waves depends critically on the predictability of the zonal index of the zonal flow in the extra-tropical region. The evolution of the latter is found to be predictable if the system does not have a large number of stable equilibrium states. (When there is only one equilibrium, the system is predictable. When there are multiple equilibria, the system is predictable provided that the initial condition is not located near one of the unstable equilibrium points.)

Our numerical solutions tentatively suggest that there are no multiple equilibria in the low-frequency portion of the large-scale flow in the atmosphere. This result implies that the variability of the extra-tropical system is probably not the result of transitions between "one or the other equilibrium states" caused by internal nonlinear dynamics of the large-scale flow only. Instead we suggest that an important cause of the low-frequency variability of the extra-tropical atmosphere may be the result of external (i.e. tropical) influence on the total *angular momentum budget* of the extra-tropical flow [Note that this mechanism is not the same as the theory of direct wave energy dispersion from the tropics (see Hoskins et al. (1977)).] Interactions between the low- and high-frequencies is another cause for the variability of the low frequencies.

It is perhaps instructive at this point to compare our result with that of Lau (1984), who finds that there is still significant variability in monthly time scales in a 15 year GCM run even in the absence of nonseasonal perturbation in the prescribed forcing such as variations in sea surface temperature, insolation and cloud cover. Lau's result suggests that some low-frequency variability in the atmosphere can be attributed to mechanisms internal to the atmosphere itself. It is not clear based on his diagnostics, however, that such mechanisms are internal to the extra-tropical system alone. In particular, there does not appear to be any ground at this point to interpret Lau's result as evidence in support of the existence of multiple equilibria in the extratropical large-scale flow. If our result of a single equilibrium is valid, then the variability found by Lau in the global atmospheric model should probably be interpreted as due to tropical influence as mentioned above and/or due to the interaction between the low and high-frequency portions of the flow.

9. Acknowledgements

This research is sponsored by the National Science Foundation under Grants ATM8023523 and ATM8217616. We are grateful to Professor W. C. Rheinboldt and J. V. Burkardt for kindly making available to us their PITCON subroutine. Helpful conversations with Dr. E. Schneider and correspondences with Professors K. Trenberth and J. Shukla are gratefully acknowledged. We should like to thank Dr. J. Alpert for making available to us the Scripps data set for the earth's topography.

10. Appendix A: Scaling analysis

10.1. Rossby number scaling

This scaling procedure can be found in most standard textbooks (see e.g. Pedlosky, 1979). It is included here for completeness.

We start with the dimensional equations for zonal and meridional momentum, continuity and temperature in log-pressure coordinates:

$$\frac{\mathrm{d}}{\mathrm{d}t}u - fv = -\frac{\partial}{\partial x}\Phi + F_x, \tag{A.1}$$

$$\frac{\mathrm{d}}{\mathrm{d}t}v + fu = -\frac{\partial}{\partial y}\Phi + F_y, \tag{A.2}$$

$$\frac{\partial}{\partial x}u + \frac{\partial}{\partial y}v + \frac{1}{\rho_0}\frac{\partial}{\partial z}(\rho_0 w) = 0, \tag{A.3}$$

$$\frac{\mathrm{d}}{\mathrm{d}t}T + w\Gamma = Q, \tag{A.4}$$

where

$$\frac{\mathrm{d}}{\mathrm{d}t} \equiv \frac{\partial}{\partial t} + u\frac{\partial}{\partial x} + v\frac{\partial}{\partial y} + w\frac{\partial}{\partial z}$$

$$\Gamma \equiv \frac{\mathrm{d}}{\mathrm{d}z}T_0 + \frac{R/c_p}{H_0}T_0,$$

F_x is the frictional force per unit mass in the x-direction,

F_y is the frictional force per unit mass in the y-direction,

Q is the diabatic heating rate/c_p, and

$$\frac{\partial}{\partial z}\Phi = \frac{R}{H_0}T.$$

Note that T is the deviation of the temperature from $T_0(z)$.

These equations are made dimensionless by scaling x, y by L. a typical horizontal length scale, z by H_0, u and v by some typical velocity U, w by $(H_0/L)\,U$, t by L/U, f by 2Ω, F by $\nu_E U/H_0^2$ and Φ by $2\Omega UL$, yielding:

$$\mathrm{Ro}\frac{\mathrm{d}}{\mathrm{d}t}u - fv = -\frac{\partial}{\partial x}\Phi + \mathrm{E}F_x, \tag{A.5}$$

$$\mathrm{Ro}\frac{\mathrm{d}}{\mathrm{d}t}v + fu = -\frac{\partial}{\partial y}\Phi + \mathrm{E}F_y, \tag{A.6}$$

for the zonal and meridional momentum equations respectively, with

$\mathrm{Ro} \equiv \dfrac{U}{2\Omega L}$ being the Rossby number and

$\mathrm{E} \equiv \dfrac{\nu_E}{2\Omega H_0^2}$ being the Ekman number.

For large-scale extra-tropical motions, it is assumed that the Ro $\ll 1$, and that E $<$ O(Ro), outside the planetary boundary layer. Expanding in asymptotic powers of Ro, one has

$$u = u_0 + \mathrm{Ro}\,u_1 + \ldots$$

$$v = v_0 + \mathrm{Ro}\,v_1 + \ldots$$

$$\Phi = \Phi_0 + \mathrm{Ro}\,\Phi_1 + \ldots$$

$$w = w_0 + \mathrm{Ro}\,w_1 + .$$

The β-plane approximation adopted here is

$$f \simeq f_0 + \mathrm{Ro}\,\beta y. \tag{A.7}$$

At the zeroeth order in Ro, (A.5) and (A.6) yield the geostrophic balance:

$$-f_0 v_0 = -\frac{\partial}{\partial x}\Phi_0 \tag{A.8}$$

$$f_0 u_0 = -\frac{\partial}{\partial y}\Phi_0. \tag{A.9}$$

These imply that

$$\frac{\partial}{\partial x}u_0 + \frac{\partial}{\partial y}v_0 = 0 \tag{A.10}$$

so

$$w_0 \equiv 0. \tag{A.11}$$

At the next order in Ro, (A.5) yields

$$\left(\frac{\partial}{\partial t} + u_0\frac{\partial}{\partial x} + v_0\frac{\partial}{\partial y}\right)u_0$$

$$-f_0 v_1 - \beta y v_0 = -\frac{\partial}{\partial x}\Phi_1, \tag{A.12}$$

and the continuity equation becomes

$$\frac{\partial}{\partial x} u_1 + \frac{\partial}{\partial y} v_1 + \frac{1}{\rho_0} \frac{\partial}{\partial z} (\rho_0 w_1) = 0. \qquad \text{(A.13)}$$

The dimensional form of (A.8) to (A.13) is used in the text.

The dimensionless form of the temperature equation is

$$\mathrm{Ro} \frac{\mathrm{d}}{\mathrm{d}t} T + \Gamma w = Q.$$

Assuming that the leading term in the expansion of Q *is* $\mathrm{Ro} Q_1$, we find that, at order Ro,

$$\left(\frac{\partial}{\partial t} + u_0 \frac{\partial}{\partial x} + v_0 \frac{\partial}{\partial y} \right) T_0 + \Gamma w_1 = Q_1. \qquad \text{(A.14)}$$

The dimensional form of (A.14) is used in the text. The prognostic form of the equations for momentum and temperature can be combined, together with the equation for continuity, to give the potential vorticity equation (3.1) for quasi-geostrophic flows.

Inside the planetary boundary layer, we assume that the frictional terms can be written, in dimensional form, as

$$F_x = \nu_E \frac{\partial^2}{\partial z^2} u,$$

$$F_y = \nu_E \frac{\partial^2}{\partial z^2} v. \qquad \text{(A.15)}$$

The horizontal diffusion terms have been neglected when compared with the vertical diffusion terms. A standard boundary layer assumption is that z should scale as $E^{1/2} H_0$, instead of just H_0 as for the case outside the boundary layer. Therefore, (A.5) and (A.6) become, inside the boundary layer,

$$\mathrm{Ro} \frac{\mathrm{d}}{\mathrm{d}t} u - fv = -\frac{\partial}{\partial x} \Phi + \frac{\partial^2}{\partial z^2} u, \qquad \text{(A.16)}$$

$$\mathrm{Ro} \frac{\mathrm{d}}{\mathrm{d}t} v + fu = -\frac{\partial}{\partial y} \Phi + \frac{\partial^2}{\partial z^2} v, \qquad \text{(A.17)}$$

in dimensionless form. To leading order in Rossby number, (A.16) and (A.17) become

$$-f_0 v = -\frac{\partial}{\partial x} \Phi + \frac{\partial^2}{\partial z^2} u, \qquad \text{(A.18)}$$

$$+ f_0 u = -\frac{\partial}{\partial y} \Phi + \frac{\partial^2}{\partial z^2} v. \qquad \text{(A.19)}$$

Using (A.8) and (A.9) to re-express the pressure gradient terms in terms of geostrophic velocities, we find

$$-f_0 (v - v_0) = \frac{\partial^2}{\partial z^2} (u - u_0), \qquad \text{(A.20)}$$

$$f_0 (u - u_0) = \frac{\partial^2}{\partial z^2} (v - v_0), \qquad \text{(A.21)}$$

assuming the geostrophic velocities are independent of height inside the boundary layer (a standard boundary layer assumption about the impressed pressure gradients).

Solving (A.20) and (A.21) in the standard manner subject to no-slip boundary condition at $z = 0$ and a no-stress condition at $z \sim z_1$ (the top of Ekman layer), we find, in dimensional form, the mass transport inside the Ekman layer:

$$-\int_0^{z_1} \bar{v} \, \mathrm{d}z = \frac{\nu_E}{f_0} \frac{\partial}{\partial z} \bar{u}_0 \Big|_0^{z_1} = -\frac{\nu_E}{f_0} \bar{u}_0(z_1) \Big/ \left(\frac{2\nu_E}{f_0} \right)^{1/2}$$

Therefore,

$$\bar{u}_0(z_1) = (f_0 \tau_E) \frac{1}{H_0} \int_0^{z_1} \bar{v} \, \mathrm{d}z \qquad \text{(A.22)}$$

If one assumes that the time-mean Hadley cell does not transport net mass across a fixed latitude, say, θ_1, then

$$\int_0^\infty \rho_0(z) \, \hat{v} \, (z) \mathrm{d}z = 0, \qquad \text{at } \theta = \theta_1,$$

which implies that the mass flow above the Ekman layer, $H_0 \langle \hat{v} \rangle$, should balance the return flow inside the Ekman layer, i.e.

$$\langle \hat{v} \rangle \Big|_{y_1} = -\frac{1}{H_0} \int_0^{z_1} \hat{v} \Big|_{y_1} \mathrm{d}z.$$

Thus

$$\hat{u}_0(y_1, z_1) = -f_0 \tau_E \langle \hat{v} \rangle |_{y_1}. \qquad \text{(A.23)}$$

This result is used in (4.9).

10.2. The time-mean equation

In Section 3, an asymptotic procedure based on the smallness of the parameter

$$\varepsilon \equiv \frac{1}{t_T(\bar{u}_o k)}$$

is used. A more formal derivation is given here.

The "fast" and "slow" nondimensional times are defined as

$$t_1 = t(k\bar{u}_0),$$

$$t_2 = t/t_T.$$

A function, such as the streamfunction Ψ, is assumed to be a function of two time variables, i.e.

$$\Psi = \Psi(t_1, t_2).$$

The running time mean

$$\hat{\Psi} \equiv \frac{1}{t_T}\int_{t-t_T/2}^{t+t_T/2} \Psi \, dt = \varepsilon \int_{t_1-1/(2\varepsilon)}^{t_1+1/(2\varepsilon)} \Psi \, dt_1$$

is taken to mean asymptotically an average over the fast time scale t_1, so that the time mean quantity, $\hat{\Psi}$, is a function of the slow time variable only, i.e.

$$\hat{\Psi} = \hat{\Psi}(t_2).$$

Therefore the dimensional form of the running time averaged potential vorticity equation is

$$\frac{1}{t_T}\frac{\partial}{\partial t_2} P\hat{\Psi} + J[\hat{\Psi}, P\hat{\Psi} + f] = f_0\left(\frac{\partial}{\partial z} - \frac{1}{H_0}\right)\hat{Q}/\Gamma - \text{TEP}. \tag{A.24}$$

If (A.24) is taken to govern the slow evolution of the quasi-stationary *waves*, then an important term in the Jacobian is the advection of potential vorticity by the zonally averaged flow

$$\bar{u}_0 \frac{\partial}{\partial x} P\hat{\Psi}, \tag{A.25}$$

which is of the order $\bar{u}_0 k$ times $P\hat{\Psi}$, where k is the typical zonal wavenumber of the large-scale quasi-stationary waves under consideration. Thus the ratio of the first to the second term in (A.24) is of the order of ε. [This result does not hold for the zonally averaged form of (A.24) because for that case (A.25) is zero, so for the mean flow equation the slow time derivative term has to be retained.] With the Jacobian term made dimensionless by $\bar{u}_0 k 2\Omega$, (A.24) becomes, in nondimensional form,

$$\varepsilon \frac{\partial}{\partial t_2} P\hat{\Psi} + J[\hat{\Psi}, P\hat{\Psi} + f] = \frac{f_0}{\bar{u}_0 k 2\Omega} \times \left(\frac{\partial}{\partial z} - \frac{1}{H_0}\right)\hat{Q}/\Gamma - \frac{\text{TEP}}{\bar{u}_0 k 2\Omega}. \tag{A.26}$$

Therefore to leading order in ε, (A.26) is

$$\bar{u}_0 k 2\Omega \, J[\hat{\Psi}^{(0)}, P\hat{\Psi}^{(0)} + f] = f_0\left(\frac{\partial}{\partial z} - \frac{1}{H_0}\right) \times \hat{Q}/\Gamma - \text{TEP}, \tag{A.27}$$

for the quasi-stationary long waves. In (A.27) we have written:

$$\hat{\Psi} = \hat{\Psi}^{(0)} + \varepsilon \hat{\Psi}^{(1)} + \ldots$$

In the absence of the slow time derivative the form of the solution, $\hat{\Psi}^{(0)}$, as a function of the slow time variable, t_2, is not determined from (A.27), but instead is determined from the lateral boundary condition in terms of $\hat{U}(t_2)$. At the next order in ε, (A.26) yields an evolution equation for $\hat{\Psi}^{(1)}$, the correction to the solution of (A.27).

11. Appendix B. Wave-mean flow interaction at channel boundaries

We examine the temperature equation:

$$\frac{\partial}{\partial t}\hat{\bar{T}} + \Gamma\hat{\bar{w}} + \frac{\partial}{\partial y}\overline{\hat{v}_0' T'} = \hat{\bar{Q}} \tag{B.1}$$

which is obtained by taking the zonal and time averages of eq. (A.14). At the lateral boundaries, the diabatic heating $\bar{Q}$, the mean circulation, $(\hat{\bar{v}}, \hat{\bar{w}})$ and the transient eddy flux, $\overline{v_0'' \hat{T}_0''}$, are specified in our model. The stationary waves can induce a change in the mean temperature there only through the part of the heat flux convergence that is due to the stationary waves:

$$\frac{\partial}{\partial y}\overline{\hat{v}_0' \cdot \hat{T}_0'}.$$

Since

$$\frac{\partial}{\partial x}\hat{\Psi} = \hat{v}_0$$

and $\hat{v}_0 = 0$ at y_1 and y_2 from the boundary condition (2.5), we find that $\hat{\Psi}$ is independent of x at these latitudes. Consequently, the zonally asymmetric part of $\hat{\Psi}$ should vanish, i.e.

$$\hat{\Psi}' \equiv \hat{\Psi} - \bar{\hat{\Psi}} = 0 \qquad \text{at } y_1 \text{ and } y_2. \tag{B.2}$$

Since (B.2) holds for all z, it then follows that

$$\hat{T}_0' \equiv \frac{f_0 H_0}{R} \frac{\partial}{\partial z} \hat{\Psi}' = 0 \qquad \text{at } y_1 \text{ and } y_2. \tag{B.3}$$

The vanishing of the perturbation meridional velocity, $\hat{v}_0'$ and the perturbation temperature, $\hat{T}_0'$, for the stationary waves implies that the eddy heat flux *convergence* due to the stationary waves should vanish and will not be able to affect the mean temperature at the lateral boundaries.

Eq. (B.1) now becomes

$$\frac{\partial}{\partial t} \bar{\hat{T}} = \bar{\hat{Q}} - \Gamma \bar{\hat{w}} - \frac{\partial}{\partial y} \overline{\hat{v}_0'' T_0''} \qquad \text{at } y_1 \text{ and } y_2. \tag{B.4}$$

The quantities in the right-hand side are all specified in our model. In particular, if they are chosen to balance each other, then (B.4) becomes

$$\frac{\partial}{\partial t} \bar{\hat{T}} = 0. \tag{B.5}$$

For this special case, the mean temperatures at the lateral boundaries, and hence the vertical shear of the zonal index, are independent of time and so are prescribed simply by the initial conditions. Our general formulation is not restricted to this special case, but (B.5) will be used in Section 7.

In most other models of stationary waves in midlatitudes, rigid channel boundaries are imposed. In such formulations, the zonal mean temperatures can evolve only in response to the mean vertical veloxity $\bar{w}$ induced by the stationary waves; the influence on the boundary temperature by the subsidence due to the Hadley circulation is ignored. While this approach has the appealing feature of being a self-contained closed system, we believe that tropical influence is more important in determining the mean-temperature at θ_1 than the mean vertical velocity induced by the stationary waves, especially when θ_1 is chosen to lie mostly in the easterly region. This then leads to our specifying the mean boundary temperature rather than predicting it using our model for the stationary waves.

Near the northern boundary θ_2, our boundary condition is more difficult to justify, as stationary waves are known to cause mean temperature changes at high latitudes (as occurring for example, during a stratospheric sudden warming). However, since mean-temperature change enters the evolution equation (4.16) only in the form of a density-weighted average, this stratospheric influence on tropospheric zonal index evolution is likely to be small. (Although *in situ* changes in the shear of the zonal index can still result (see eq. (4.13)), sensitivity studies that we have carried out for different vertical shears of zonal index suggest that the predictability of the surface zonal index is scarcely affected. In particular no new equilibrium is created.) Therefore our conclusions concerning predictability of the stationary waves should probably not be affected by our boundary condition at θ_2.

List of symbols

$\bar{(\ )}$: zonal average

$(\ )'$: $(\ ) - \bar{(\ )}$, deviation from zonal mean

$\hat{(\ )}$: running time mean

$(\ )''$: $(\ ) - \hat{(\ )}$, transient eddies

$\langle(\ )\rangle$: density-weighted vertical integral from z_1 to ∞

y: $a\theta$, where a is the earth's radius and θ is latitude

y_1, y_2: $a\theta_1, a\theta_2$, the locations forming the channel boundaries

z: $H_0 \ln\left(\frac{p_0}{p}\right)$

H_0: the scale height, ~ 8 km, at the lower boundary

z_1: height of the Ekman boundary layer

u_0, v_0: geostrophic velocities

u_1, v_1: ageostrophic velocities

U: net geostrophic zonal flow between y_1 and y_2, also called the zonal index

U_0 $\hat{U}(z_1, t)$

U^*: zonal momentum driving for $\langle \hat{U} \rangle$

$U^\dagger$: zonal driving for U_0 in the angular momentum budget at z_1

$\rho_0(z)$: $\rho_0(0)e^{-z/H_0}$

$T_0(z)$: basic state temperature profile

T: deviation of temperature from T_0

Q: diabatic heating rate per unit mass divided by c_p, the specific heat at constant pressure

κ: ratio of the mean zonal wind at the "surface" to that at the equivalent barotropic level for the mean flow

TEP: transient eddy flux convergence of potential vorticity

TEH: transient eddy flux convergence of heat.

REFERENCES

Charney, J. G. and Eliassen, A. 1949. A numerical method for predicting the perturbations of the middle latitude westerlies. *Tellus 1*, 38–54.

Charney, J. G. 1960. Numerical prediction and the general circulation, in *Dynamics of climate*, 12–17 R. L. Pfeffer, ed. Pergamon Press.

Charney, J. G. and Drazin, P. G. 1961. Propagation of planetary-scale disturbances from the lower into the upper atmosphere. *J. Geophys. Res. 66* 83–109.

Charney, J. G. and DeVore, J. G. 1979. Multiple flow equilibria in the atmosphere and blocking. *J. Atmos. Sci. 36*, 1205–1216.

Charney, J. G., Shukla, J. and Mo, K. C. 1981. Comparison of a barotropic blocking theory with observation. *J. Atmos. Sci. 38*, 762–779.

Charney, J. G. and Straus, D. M. 1980. Form-drag instability, multiple equilibria and propagating planetary waves in baroclinic orographically forced planetary wave systems. *J. Atmos. Sci. 37*, 1157–1176.

Egger, J. and Schilling, H. D. 1984. Predictability of atmospheric low-frequency motions, in *Predictability of fluid motions*, G. Holloway and B. J. West (eds). American Institute of Physics, 612 pages.

Gall, R., Blakeslee, R. and Somerville, R. C. J. 1979. Cyclone-scale forcing of ultralong waves. *J. Atmos. Sci. 36*, 1692–1698.

Gates, W. L. and Nelson, A. B. 1975. A new (revised) tabulation of Scripps topography on a 1° global grid. Part I: Terrain heights. The Rand Corporation, Ro-1276-1-ARPA, 140 pp.

Geller, M. A., Wu, M. F. and Gelman, M. E. 1984. Troposphere-stratosphere (surface-55 km) monthly winter general circulation statistics for the northern hemisphere: interannual variations. *J. Atmos. Sci. 41*, 1726–1744.

Hansen, A. R. and Chen, T. C. 1982. A spectral energetics analysis of atmospheric blocking. *Mon. Wea. Rev. 110*, 1146–1165.

Hansen, A. R. and Sutera, A. 1984. A comparison of the spectral energy and enstrophy budgets of blocking versus nonblocking periods. *Tellus 36A*, 52–63.

Hoskins, B. J., Simmons, A. J. and Andrews, D. G. 1977. Energy dispersion in a barotropic atmosphere. *Q. J. R. Meteorol. Soc. 108*, 553–567.

Jacqmin, D. A. 1983. The causation and variability of the northern winter quasi-stationary planetary waves. Harvard University Ph.D. Thesis. Cambridge, MA 02138, U.S.A.

Jacqmin, D. A. and Lindzen, R. S. 1985. The causation and sensitivity of the Northern Winter planetary waves. *J. Atmos. Sci. 42*, 724–745.

Källén, E. 1983. A note on orographically induced instabilities in two-layer models. *J. Atmos. Sci. 40*, 500–505.

Lau, N.-C. 1979. The observed structure of tropospheric stationary waves and the local balances of vorticity and heat. *J. Atmos. Sci. 36*, 996–1016.

Lau, N.-C. 1984. Circulation statistics based on FGGE level III-B analysis produced by GFDG. NOAA Data Report ERL GFDL-5, 427 pages.

Lau, N.-C. and Wallace, J. M. 1979. On the distribution of horizontal transports by transient eddies in the Northern Hemisphere wintertime circulation. *J. Atmos. Sci. 36*, 1844–1861.

Lorenz, E. N. 1963. Deterministic neoperiodic flow. *J. Atmos. Sci. 20*, 130–141.

Lorenz, E. N. 1965. A study of the predictability of a 28-variable atmospheric model. *Tellus 17*, 321–333.

Lorenz, E. N. 1982. Atmospheric predictability with a large numerical model. *Tellus 34*, 505–513.

Matsuno, T., 1970. Vertical propagation of stationary planetary waves in the winter Northern Hemisphere. *J. Atmos. Sci. 27*, 871–883.

Namias, J. 1947. Physical nature of some fluctuations in the speed of the zonal circulation. *J. Meteorol. 4*, 125–133.

Oort, A. H. 1983. *Global atmospheric circulation statistics*, 1958–1973. NOAA Professional Paper No. 14, U.S. Govt. Printing Office, Washington, DC, USA, 180 pp.

Opsteegh, J. D. and van den Dool, H. M. 1979. A diagnostic study of the time-mean atmosphere over Northwestern Europe during winter. *J. Atmos. Sci. 36*, 1862–1879.

Pedlosky, J. 1979. *Geophysical fluid dynamics*. Springer-Verlag, 624 pp.

Rambaldi, S. 1982. Multiple equilibria and their stability in a barotropic and baroclinic atmosphere. Ph.D. Thesis, M.I.T., Cambridge, MA 02139.

Reinhold, B. B. and Pierrehumbert, R. T. 1982. Dynamics of weather regimes: Quasi-stationary waves and blocking. *Mon. Wea. Rev. 110*, 1105–1145.

Rheinholdt W. C. and Burkardt, J. V. 1983a. A locally parameterized continuation process. *A. C. M. Trans. Math Software 9*, 215–235.

Rheinboldt, W. C. and Burkardt, J. V. 1983b. A program for a locally parameterized continuation process. *A. C. M. Trans. Math. Software 9*, 236–241.

Roads, J. O. 1980. Stable near-resonant states forced by orography in a simple baroclinic model. *J. Atmos. Sci. 37*, 2381–2395.

Roads, J. O. 1980. Climatic-anomaly experiments in middle-latitudes. *Tellus 32*, 410–427.

Rossby, C.-G. and collaborators 1939. Relation between variations in the intensity of the zonal circulation of the atmosphere and the displacements of the semi-permanent centers of action. *J. Marine Res. 2*, 38–55.

Shukla, J. 1981. Dynamical predictability of monthly means, *J. Atmos. Sci. 38*, 2547–2572.

Shukla, J. 1984. The predictability of time averages: Part II. The influence of boundary forcings, in *Problems and prospects in long and medium range forecasting*, D. M. Burridge and E. Källén (eds), pp. 155–206. Springer-Verlag.

Smagorinsky, J. 1969. Problems and promises of deterministic extended range forecasting. *Bull. Amer. Meteorol. Soc. 50*, 286–311.

Tung, K. K. 1983. On the nonlinear versus linearized lower boundary conditions for topographically forced stationary long waves. *Mon. Wea. Rev. 111*, 60–66.

Tung, K. K. and Lindzen, R. S. 1979a. A theory of stationary long waves, Part I: A simple theory of blocking. *Mon. Wea. Rev. 107*, 714–734.

Tung, K. K. and Lindzen, R. S. 1979b. A theory of stationary long waves, Part II. Resonant Rossby waves in the presence of realistic vertical shears. *Mon. Wea. Rev. 107*, 735–750.

Tung, K. K. and Rosenthal, A. J. 1985. Theories of multiple equilibria, a critical reexamination. Part 1: Barotropic models. *J. Atmos. Sci. 42*, 2804–2819.

Wallace, J. M. 1983. The climatological mean stationary waves: observational evidence, in *Large-scale dynamical processes in the atmosphere*, B. J. Hoskins and R. P. Pearce (eds). Academic Press, 27–53.